Master's Thesis in FMH606 2016

Nora Cecilie Ivarsdatter Furuvik

Simulation of oil production and CO_2-distribution in carbonate reservoir

Telemark University College
Faculty of Technology
Department of Process, Energy and Environmental Technology
Kjølnes ring 56
3918 Porsgrunn

http://www.hit.no

Telemark University College
Faculty of Technology
M.Sc. Programme

MASTER'S THESIS, COURSE CODE FMH606

Student:	**Nora Cecilie Ivarsdsatter Furuvik**
Thesis title:	**Simulation of oil production and CO_2-distribution in a carbonate reservoir**
Signature:	. . . . .
Number of pages:	65 + Appendices
Keywords:	**CO_2-EOR, CO_2-distribution, Oil production**
	Carbonate reservoir, Petrophysics, OLGA/Rocx
Supervisor:	Britt M. E. Moldestad Sign.: . . . . .
2nd supervisor:	Haavard Aakre Sign.: . . . . .
Censor:	Christoph Pfeifer Sign.: . . . . .
External partner:	InflowControl AS
Availability:	Open

Archive approval (supervisor signature)**:** Sign.: . . . . . **Date :** . . . . . .

Abstract:

Deep geologic injection of supercritical carbon dioxide (CO_2) for enhanced oil recovery (EOR), plays an important role in the sequestration of CO_2 to minimize the impact of CO_2-emissions due to global warming. CO_2-EOR refers to the oil recovery technique where supercritical CO_2 is injected to the reservoirs to stimulate oil production from depleted oilfields. The CO_2 mixes with the stranded oil, not producible by primary and secondary oil recovery techniques, changing the oil property and making the immobile oil mobile and producible.

The objective of this Master's thesis was to study CO_2-injection into a carbonate reservoir. The study includes near-well simulations of oil production and CO_2-distribution, using the reservoir software Rocx in combination with OLGA.

CO_2-injection into a carbonate reservoir increases the oil recovery, but simultaneously the water production is increased.

Carbonate reservoirs with fractures have low oil production, high water production, early water breakthrough and high water cut.

Water breakthrough occurs after only 2.9 days in the fractured reservoir, and the water cut is 97.5 %. Closing the fractured zone causes delayed water breakthrough and dramatically reduced water cut, resulting in improved oil recovery as well as lower production and separation costs.

The simulations indicate that CO_2-injection into a carbonated reservoir in combination with closing fractured zone result in good distribution in the reservoir.

Sammendrag (in Norwegian)

Hensikten med denne oppgaven var å se på hvordan CO_2-injeksjon påvirker oljeproduksjonen, og samtidig studere hvordan CO_2 distribueres i et karbonat reservoar. Det ble utført simuleringer ved hjelp av simuleringsprogrammet OLGA/Rocx.

Injeksjon av superkritisk CO_2 i dype geologiske formasjoner (CO_2- EOR), spiller en viktig rolle i lagringen av CO_2 for å redusere global oppvarming. CO_2-EOR omhandler injeksjon av superkritisk CO_2 for å forbedre oljeutvinningen fra utarmede oljefelt. CO_2 blander seg med den olje, som ikke er produserbar ved primære eller sekundære oljeutvinningsmetoder, og endre de fysiske egenskapene til oljen slik at oljen blir mer mobil.

Resultatene fra simuleringene viser at CO_2-injekson i et karbonat reservoar fører til økt oljeutvinning, men samtidig økt vannproduksjon. Karbonat reservoar med sprekk har lav oljeproduksjon, høy vannproduksjon, tidlig vanngjennombrudd og høyt vann kutt.

Vanngjennombruddet oppstår allerede etter 2.9 dager i reservoar med sprekk, og vannkuttet er 97,5%. Ved å stenge den delen av reservoaret som har sprekk, vil vanngjennombruddet bli forsinket og vannkuttet redusert. Dette medfører en forbedret oljeproduksjon, samt lavere separasjons- og produksjonskostnader.

CO_2-injeksjon i et karbonat reservoar der den delen med sprekk er stengt gir god fordeling I reservoaret.

Contents

Sammendrag (in Norwegian) 4

Contents 5

Preface 7

Nomenclature list 8

List of figures 11

List of tables 13

1 Introduction 14

2 Oil recovery and CO_2-injection 16

2.1 CO_2-EOR 17

2.2 CO_2-storage in deep saline aquifers 18

3 Petrophysical properties in hydrocarbon reservoirs 19

3.1 Hydrocarbon reservoir 19

3.2 Porosity 20

3.2.1 Sorting of grains 22

3.2.2 Grain shape 23

3.2.3 Packing arrangement of grains 24

3.2.4 Degree of cementation 24

3.3 Saturation 25

3.4 Wettability 26

3.4.1 Interfacial tension 27

3.4.2 Capillary Pressure 27

3.5 Permeability 30

3.5.1 Relative permeability 32

3.5.2 Relation between porosity and permeability of a reservoir rock 34

4 Carbonate reservoirs 36

4.1 Petro physical properties of carbonate reservoirs 36

5 Simulation of oil production and CO_2 distribution in carbonate reservoir 38

5.1 Simulation software OLGA/Rocx 38

5.2 Simulation cases 40

5.2.1 Relative permeability curves 41

5.2.2 Input to OLGA and Rocx 44

6 Results 46

6.1 Oil production from a homogenous carbonate reservoir 46
6.2 Oil production from a carbonate reservoir with fracture 48
6.3 Oil production from a heterogeneous carbonate reservoir with closed valve in the fractured zone 51
6.4 CO_2 distribution in a carbonate reservoir rock 53
6.4.1 Distribution of CO_2 and water after water breakthrough 53
6.4.2 Distribution of CO_2 and water after 400 days 55
7 Discussion 57
8 Conclusion 60
9 References 61
Appendices 65

Preface

This Master's thesis is the result of the coarse FMH606 at Telemark University College, Faculty of Technology in Porsgrunn.

I would like to thank my supervisor Britt Margrethe Emilie Moldestad for good help and advices during the project.

Task description is found in appendix A.

Paper published in *Linköping Electronic Conference Proceedings 2015 (119) s. 347-355* is found in Appendix B. Title: Simulation of CO_2 injection in oil reservoir

Porsgrunn, 03.02.2016

Nora Cecilie Ivarsdatter Furuvik

Nomenclature list

Abbreviation	Description	Unit
A	Fluid flow area	[cm^2]
AICV	Autonomous Inflow Control Valve	[-]
cP	Centipoise, (1 cP = 1 m Pa·s)	[-]
D	Darcy, Unit for Permeability	[mD]
EOR	Enhanced Oil Recovery	[-]
ICD	Inflow Control Device	[-]
$\boldsymbol{K}$	Permeability	[mD]
$\boldsymbol{K_g}$	Effective permeability to gas phase	[mD]
$\boldsymbol{K_i}$	Effective permeability to fluid phase *i*	[mD]
$\boldsymbol{K_o}$	Effective permeability to oil phase	[mD]
$\boldsymbol{K_{ri}}$	Relative permeability to fluid phase *i*	[-]
$\boldsymbol{K_{ro}}$	Relative permeability to oil phase	[-]
$\boldsymbol{K_{rocw}}$	Relative permeability to oil at irreducible water saturation	[-]
$\boldsymbol{K_{rwro}}$	Relative permeability to water at residual oil saturation	[-]
$\boldsymbol{K_{rw}}$	Relative permeability to water phase	[-]
$\boldsymbol{K_w}$	Effective permeability to water phase	[mD]
$\boldsymbol{n_w}$	Corey coefficient for water	[-]
$\boldsymbol{n_{ow}}$	Corey coefficient of oil	[-]
$\boldsymbol{S}$	Saturation	[fraction]
$\boldsymbol{S_{gas}}$	Gas saturation	[fraction]
$\boldsymbol{S_{oil}}$	Oil saturation	[fraction]
$\boldsymbol{S_{or}}$	Residual oil saturation	[fraction]
$\boldsymbol{S_{water}}$	Water saturation	[fraction]

S_{wc}	Irreducible water saturation	[fraction]
Sm^3	Standard cubic meter (cubic meter at t=15° and p=1,01325 barA)	[-]
V_{gas}	Pore volume occupied by gas	[cm^3]
V_{oil}	Pore volume occupied by oil	[cm^3]
V_{total}	Total pore volume in the reservoir	[cm^3]
V_{water}	Pore volume occupied by water	[cm^3]
$\mathbf{P_c}$	Capillary pressure	[psi]
$\mathbf{P_{nw}}$	Capillary pressure in the non-wetting phase	[psi]
$\mathbf{P_w}$	Capillary pressure in the wetting phase	[psi]
Q	Volumetric fluid flow rate	$[\frac{cm^3}{s}]$
Q_i	Volumetric fluid flow rate of fluid phase *i*	$[\frac{cm^3}{s}]$
r	Pore radius	[..]
$\frac{dp}{dx}$	Pressure drop over a flow length *x*	$[\frac{atm}{cm}]$
$\frac{dp_i}{dx}$	Pressure drop over a flow length *x* for fluid phase *i*	$[\frac{atm}{cm}]$

Greek letters	**Description**	**Unit**
$\mathbf{\Phi}$	Effective porosity	[fraction]
$\boldsymbol{\phi_a}$	Absolute porosity	[fraction]
μ	Viscosity of the fluid	[cP]
μ_i	Viscosity of the fluid fluid phase *i*	[cP]
$\boldsymbol{\sigma}$	Interfacial tension between two fluid phases	$[\frac{dynes}{cm}]$
$\boldsymbol{\sigma_{nw}}$	Interfacial tension between non-wetting and wetting fluid	$[\frac{dynes}{cm}]$
$\boldsymbol{\sigma_{os}}$	Interfacial tension between oil and surface	$[\frac{dynes}{cm}]$
$\boldsymbol{\sigma_{ow}}$	Interfacial tension between oil and water	$[\frac{dynes}{cm}]$

$\boldsymbol{\sigma_{ws}}$	Interfacial energy between water and surface	$[\frac{dynes}{cm}]$
$\boldsymbol{\theta}$	Contact angle between the surface and the fluid phase	[°]

List of figures

Figure 2-1	Primary, secondary and tertiary oil production	15
Figure 2-2	Principle of CO_2-EOR	16
Figure 3-1	Formation process of crude oil and natural gas	18
Figure 3-2	Segregation of oil, gas and water in a reservoir	19
Figure 3-3	Representation of voids	20
Figure 3-4	Three basic types of pores	20
Figure 3-5	Type of pores and porosity of a reservoir rock	21
Figure 3-6	Sorting of grains	22
Figure 3-7	Varying roundness and sphericity of mineral grains	23
Figure 3-8	Cubic and rhombohedral packing of spheres	23
Figure 3-9	Compaction and sedimentation of sediments	24
Figure 3-10	Wetting in pores	26
Figure 3-11	Wettability in a reservoir rock	27
Figure 3-12	Capillary pressure in a tube	28
Figure 3-13	The interface between two immiscible fluids	28
Figure 3-14	Relationship between the pore size distribution and the capillary pressure curve	29
Figure 3-15	Relation between fluid flow and rock permeability	30
Figure 3-16	Relative permeability curve in water-wet rock	32
Figure 3-17	Relative permeability curves in oil-wet rock	32
Figure 3-18	Relationship between porosity and permeability	34
Figure 5-1	Grid and geometry of the simulated reservoir	37
Figure 5-2	OLGA Study Case for performed simulations	38
Figure 5-3	A schematic of the pipe and the annulus	39
Figure 5-4	Near-well simulation in OLGA	39
Figure 5-5	Relative permeability curves with variable Values for the Corey's exponent	41
Figure 5-6	Relative permeability curves in oil-wet reservoir	43
Figure 6-1	Accumulated oil and water, Base Case 1 and Base Case 2	45
Figure 6-2	Volumetric flowrate of oil and water, Base Case 1 and Base Case 2	46
Figure 6-3	Total liquid volumetric flowrate in pipe, Base Case 2	47

Figure 6-4	Accumulated oil and water, Case 1 and Case 2	48
Figure 6-5	Total liquid volumetric flowrate in pipe, Case 2	49
Figure 6-6	Graphical output of the water cut, Case 2	49
Figure 6-7	Accumulated oil and water, Case 3 and Case 4	50
Figure 6-8	Total liquid volumetric flowrate in pipe, Case 4	51
Figure 6-9	Graphical output of the water cut, Case 3 and Case 4	52
Figure 6-10	Oil fraction scale used in the results generated by Techplot	53
Figure 6-11	Saturation of oil initially and at water breakthrough	54
Figure 6-12	2D view at water breakthrough in the second production zone	55
Figure 6-13	Saturation of oil after 400 days	55
Figure 6-14	2D view in the second production zone after 400 days of production	56
Figure 7-1	Accumulated oil volume, Case 2 and Case 4	58
Figure 7-2	Accumulated water volume, Case 2 and Case 4	58
Figure 7-3	Total liquid flowrate along the pipe, Case 2 and Case 4	59
Figure 7-4	Water cut, Case 2 and Case 4	59

List of tables

Table 3-1	Relative permeability characteristics of oil-wet and water-wet reservoirs	33
Table 4-1	Petro physical properties of carbonate reservoirs	36
Table 5-1	Reservoir and fluid properties for the specific simulations	38
Table 5-2	Simulation cases	40
Table 5-3	Corey coefficient in oil-wet reservoirs	41
Table 5-4	Relative permeability data for specific simulation cases	42
Table 5-5	Input for the performed simulations	44
Table 7-1	Summarize of results from the different cases	56

1 Introduction

Deep geologic injection of supercritical carbon dioxide (CO_2) for enhanced oil recovery (EOR), plays an important role in the sequestration of CO_2 to minimize the impact of CO_2-emissions due to global warming. [1], [2]

Sequestration of CO_2 in subsurface geological formations and deep saline aquifers assures long-term containment of CO_2 for atmospheric purposes. Besides the geochemical reactions that occur between the multiphase fluids and the minerals in the geological formation, the CO_2 sequestration process induces complex phase behaviors of CO_2 with oil. [2], [3]

CO_2-EOR refers to the oil recovery technique where supercritical CO_2 is injected to the reservoirs to stimulate oil production from depleted oilfields. The CO_2 mixes with the stranded oil, not producible by primary and secondary oil recovery techniques, changing the oil property and making the immobile oil mobile and producible. CO_2-injection has been successfully used for EOR since early 1970's. [1]

Integrating CO_2 sequestration and CO_2-EOR increases the CO_2-storage potential at the same time stimulates to oil production from depleted reservoir. Advanced carbon capture technology used in the petroleum industry holds the promise for reducing the carbon footprint from industrial sources. The CO_2 produced along with the oil ends up trapped by physical and capillary mechanisms and will remain sequestered at the depth. At the production facility CO_2 is separated from the oil and the water. The oil is sold, the water is recycled and the CO_2 is compressed and readied for underground reinjection and recycling. [1], [2]

Hydrocarbon reservoirs are porous and permeable rocks composed of mineral grains and crystals. Thus the efficiency of the CO_2-EOR technique greatly depends on the reservoir characteristics, the nature of the displacing process and the displaced fluid. These reservoir characteristics include petrophysical properties like porosity, wettability, capillary pressure, relative permeability and the degree of reservoir homogeneity. [1], [4]

Water is present in every hydrocarbon reservoir and is the most abundant fluid in the ground. During oil recovery processes, a certain amount of water always comes with the main stream from the recovery well. Today oil companies produce an average of three barrels of water for each barrel of oil from their depleting reservoirs. [4] For the oil company this is both economic, operational and environmental challenging. The oil industry aim for new inflow technology to minimize the water production from the reservoirs. [4] The Norwegian company InflowControl AS has developed an Autonomous Inflow Control Valve (AICV)

that can replace the conventional Inflow Control devices (ICD) installed in a well. The AICV will automatically shut off the production of water from one specific zone in the well, but at the same time the production of oil will continue from other zones. [5]

This study focuses on CO_2-storage and CO_2-EOR in a fractured carbonate reservoir, and includes simulations of oil production and CO_2-distribution in the reservoir. In carbonate reservoirs, porosity varies from 1% to 35%, with typically 10% - 15%. Carbonate reservoirs are characterized by low permeability and strong heterogeneity, causing significant amounts of CO_2 to be recycled when CO_2 is reinjected into the reservoir. The oil production performance from carbonate reservoirs is nearly half the production from other reservoir rocks, whereas the CO_2 utilization is about 60% less. [6], [1]

This work is primarily divided into two sections: First, the study of the petrophysical properties of hydrocarbon reservoirs and the related reservoir properties for carbonate reservoirs. Second, near-well simulations of oil production and near-well simulation of CO_2-injection into a carbonate reservoir rock. The simulations are carried out for an oil-wet carbonate reservoir rock with fractures.

The reservoir simulation software Rocx in combination with OLGA are used in the performance of the simulations.

2 Oil recovery and CO_2-injection

Oil recovery refers to the extraction process of liquid hydrocarbons from beneath the Earth's surface. The extraction process occurs in three different phases; primary, secondary and tertiary oil recovery phase. The three different methods of oil production are illustrated in Figure 2-1. [7]

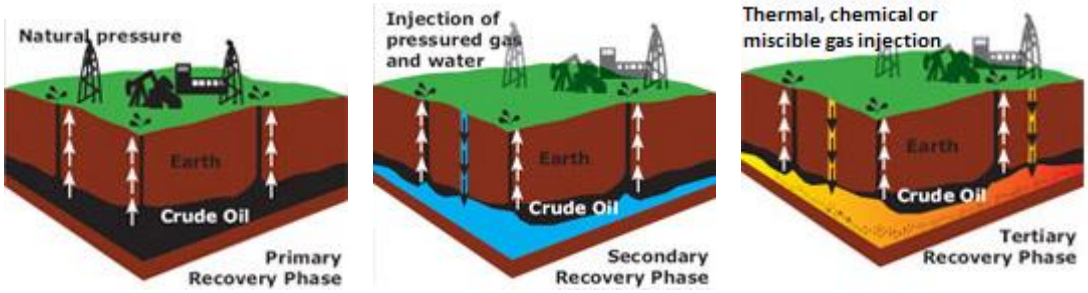

Figure 2-1: Primary, secondary and tertiary oil production. [7]

In the primary phase of oil production, the drive mechanism for oil extraction is the natural pressure difference between the reservoir and the production well. The reservoir covers an extended area, thus the reservoir pressure slowly will decrease and the oil production starts to decline. The main pressure drop is located near the production well. To re-pressurize the reservoir and drive out the remaining oil, a secondary oil recovery phase is applied. In this method pressurized gas and/or water is injected into the reservoir to give artificial pressure to trapped oil, sweeping more oil towards the production well. After primary and secondary oil recovery phases, there are still large amounts of oil remained trapped in the reservoir. [8] The traditional primary and secondary oil recovery phase produces one third of the oil in place while two third still are left behind in the reservoirs. [4] The remaining oil reserves are trapped in the reservoir pores, by capillary forces and can no longer be forced to migrate towards the production well by water flooding. For recovery of the remaining oil, a tertiary phase of oil production is used. [2], [9], [8] Tertiary enhanced oil recovery (EOR) involves a technique for injection of steam (thermal recovery), chemicals (chemical flooding) or miscible gasses (miscible displacement) to improve the properties of the remaining oil in order to make it flow more freely within the reservoir. [2], [9] One of the most proven tertiary oil recovery phases is flooding of CO_2, commonly referred to CO_2-EOR (CO_2-Enhanced Oil Recovery).

2.1 CO_2-EOR

CO_2-EOR is a technique that involves injection of supercritical CO_2 into underground geological formations, or deep saline aquifers. The goal is to revitalize matured oilfields, allowing them to produce additional oil. CO_2 is highly soluble in oil and to a lesser extent in water. As CO_2 migrates through the reservoir rock, it mixes with the residual oil trapped in the reservoir pores, enabling the oil to slip through the pores and sweep up in the flow from the CO_2-injection well towards the recovery well. [2] The principle of CO_2-EOR is shown in Figure 2-2.

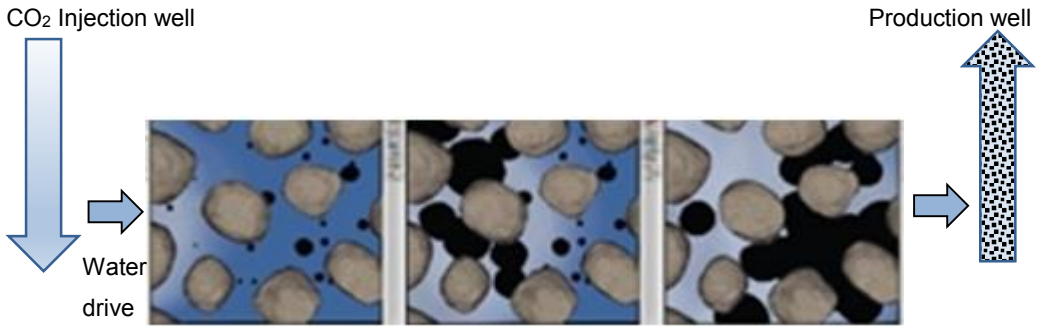

Figure 2-2: Principle of CO_2-EOR. [10]

CO_2 is injected into the oil formation and encounters the oil trapped in the reservoir rock pores. CO_2 and oil mix, leading to expansion of the oil. The oil becomes less viscous and moves toward the producing well.

When supercritical CO_2 and oil mix, a complicated series of interactions occur wherein the mobility of the crude oil is increased. These interactions involve reduction in the interfacial tensions and the capillary pressure between the oil and the water phase. Injection of CO_2 into the oil formation changes the oil physical properties in two ways, leading to enhanced oil recovery. First, reduction in oil viscosity so that the oil flows more freely within the reservoir. Second, a process of dissolution thereby causing swelling of the oil, resulting in expansion in oil volume which means that some fluid have to migrate. The amount of swelling depends on the reservoir pressure and temperature, the hydrocarbon composition and the physical properties of the oil. [11], [12], [2], [13]

Use of supercritical CO_2 for EOR increases the oil production, simultaneously contributing to minimize the impact of CO_2-emission to the atmosphere. The injected CO_2 remains trapped in the underground geological formations, as much of the CO_2 injected is exchanged for the oil and water in the pores. [12]

2.2 CO_2-storage in deep saline aquifers

At sufficiently high pressure, CO_2 achieves miscibility with oil. Complete miscibility between the oil and the CO_2 reduces interfacial tension and capillary forces, and could help recover in theory all of the residual oil. [11]

Under favorable conditions, the CO_2 becomes supercritical. In this phase the CO_2 is more dense than the gaseous CO_2, but less dense and viscos than the reservoir fluids. Due to density difference, the supercritical CO_2 tends to migrate towards the upper layer of the reservoir. The CO_2-flow is controlled by its phase behavior with the resident fluids, involving multiple liquid and vapor phases. These complex interactions can create unexpected recovery patterns. [12], [11] The preferred depths to inject CO_2 is greater than 800 meters, as it provide the required conditions above the critical point of CO_2. At these conditions, the CO_2 is kept in a supercritical phase which increases the storage capacity of the formation, because more CO_2 can be stored within a specific volume. [12] Supercritical CO_2 fills less than 1 % volume compared to gaseous CO_2.

Sequestration of CO_2 in deep geological formations is an important aspect in minimizing the atmospheric emissions of CO_2. CO_2 can be stored in deep saline aquifers as free CO_2, most likely as a supercritical phase in the pores of the reservoir rock, as a dissolved phase in the formation water or CO_2 converted to rock matrix. [11]

The volume available for storage depends on the reservoir structure, porosity and permeability. The CO_2-injection into the deep geological formations is affected by the heterogenetic in the formation. CO_2-storage capacity depends on the presence of faults and fractures, since they have a great impact on the fluid flow in the reservoir. [11]

3 Petrophysical properties in hydrocarbon reservoirs

Petrophysic is the study of the porous geological formations, their physical properties and the interactions between the rock and the fluids. [14] This chapter gives an introduction to the fundamentals of the petrophysic, and is designed to provide basic understanding of the characteristics of a reservoir rock and the multiphase fluid flow within the reservoir.

3.1 Hydrocarbon reservoir

Crude oil and natural gas are both mixtures of liquid hydrocarbons that exist naturally in the Earth's bedrock. In general, crude oil and natural gas are not formed in the reservoir rock from which they are produced. They are generated in a source rock, through heating and compression of organic materials for thousands of years. Figure 3-1 illustrates the formation process of hydrocarbons in a reservoir rock.

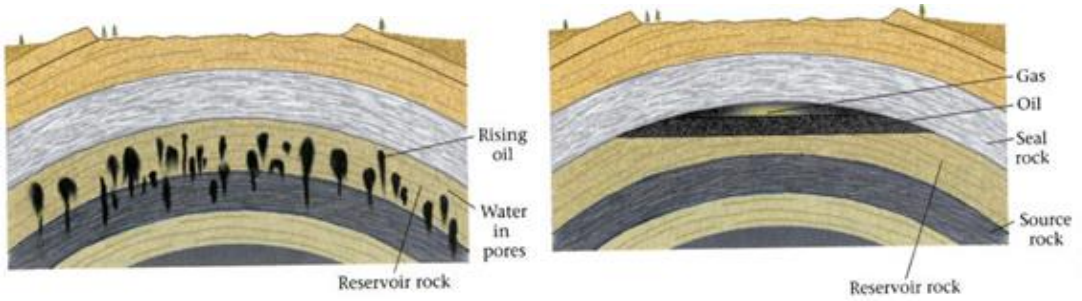

Figure 3-1: Formation process of crude oil and natural gas. [16]

Since hydrocarbons are light in density, the hydrocarbons start to migrate in a porous source rock containing water. The hydrocarbons move through fault and fractures in the source rock until they are trapped in a reservoir rock. The reservoir rock is overlain by a seal rock, an impermeable rock layer that does not allow fluids to flow through. The oil and gas accumulate in the trap, forming the hydrocarbon reservoir. If there is no such trap along the migration route, the oil and gas will continue their migration out onto the surface of the Earth. [15], [16]

Accumulation of hydrocarbons in such traps are usually found in permeable and porous sedimentary rocks. Since the pores are initially water-saturated, the migration of the hydrocarbons takes place in an aqueous environment. The oil, gas and formation water will separate in different layers once they are caught in the trap. The segregation of the fluids occur according to density difference. A cross section of a hydrocarbon reservoir showing vertical segregation of oil, gas and water is shown in Figure 3-2.

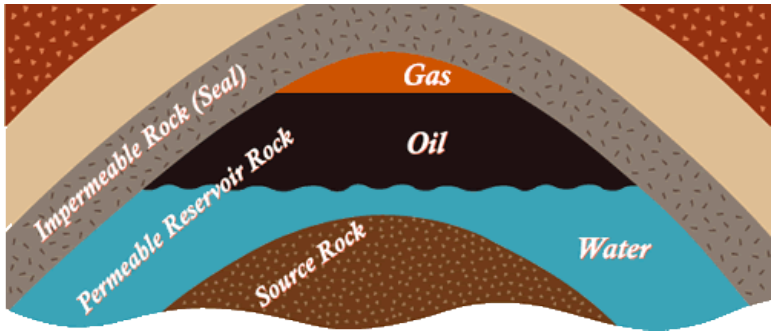

Figure 3-2: Segregation of oil, gas and water in a reservoir. [19]

Gas will accumulate in the highest portion of the trap, forming a free gas cap. Oil accumulates in the middle of the trap, forming an oil reservoir. Water goes to the bottom, this is due to the specific gravity for water is higher than for oil. Because hydrocarbon reservoirs consist of voids and tiny openings in the rock, capillary forces acting between the fluids resist complete gravitational segregation of the fluid phases. Therefore, water is always found in small amounts in all zones of the reservoir. [15], [17], [16], [18]

For a rock to act as a reservoir, it must have pores to store fluid and the pores must be connected to allow transmission of the fluids. [14] The reservoir rock is composed of mineral grains and crystals, hence the petrophysical properties of the reservoir is highly dependent on the properties of the minerals. Porosity, saturation, wettability and relative permeability are the physical parameters that directly influence the oil recovery processes as they all control the distribution of the fluids. [3]

3.2 Porosity

A porous rock consists of mineral grains and small spaces in between the grains, called voids or pores. Figure 3-3 illustrates the mineral grains and the pores, and their distribution in the reservoir rock.

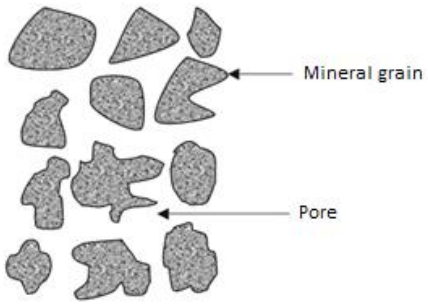

Figure 3-3: Representation of voids. [20]

In the reservoir rock the pores are of different shapes and sizes, some of them are too small to be seen and some appear as fractures or tiny cracks in the rock. All porous materials have three basic types of pores: catenary pores, cul-de-sac pores and closed pores. [18], [21], [9] A diagrammatic representation of the three different pore types is shown in Figure 3-4.

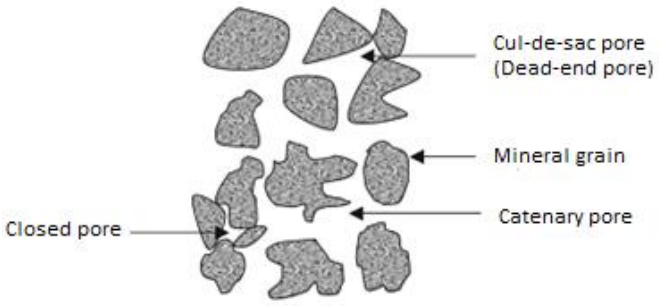

Figure 3-4: Three basic types of pores. [20]

Catenary pores are pores connected to other pores with more than one pore channel. The catenary pores are the ideal pores considering oil recovery processes, this is because oil easily can be flushed from these pores by secondary and tertiary oil recovery techniques. Cul-de-sac pores (dead-end pores) include the pores that are only connected to other pores through one pore channel, while closed pores refer to the pores that have no connection to other pores at all. Closed pores are completely isolated from the pore network. [20]

Porosity might be absolute, effective or ineffective. Catenary pores and dead-end pores represent the effective porosity. Even if dead-end pores cannot be flushed out, they can still produce oil by pressure depletion or gas expansion. Closed pores are ineffective because no oil can move neither in nor out of the pores. Figure 3-5 shows how the absolute porosity, the effective porosity and the ineffective porosity are distinguished by their access capabilities to the reservoir fluids. [18]

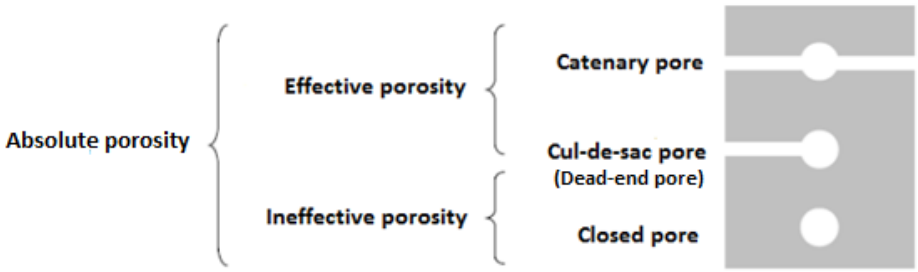

Figure 3-5: Type of pores and porosity in a reservoir rock [18]

The porosity in a reservoir represents the measure of the pores within the porous material. Absolute porosity encompasses all the pores, including interconnected pores as well as those pores that are totally sealed off. The absolute porosity is termed ϕ_a and is defined as the

ratio of total pore volume (catenary pores, dead-end pores and closed pores) to the total volume of the porous rock. [3], [20] The mathematical expression for absolute porosity is:

$$\phi_a = \frac{Total\ pore\ volume}{Total\ volume} \qquad [3\text{-}1]$$

Effective porosity (ϕ) is the fraction of pores in which fluid can flow, and it is the proportion of pores that exclude the completely disconnected pores (closed pores). Effective porosity is defined as the ratio of the interconnected pore volume (catenary pores and dead-end pores) to the total volume of the porous rock. Thus, the effective porosity measures the pores that are interconnected to the surface:

$$\phi = \frac{Pore\ volume\ of\ interconnected\ pores}{Total\ volume} \qquad [3\text{-}2]$$

The difference between absolute and effective porosity is the ineffective porosity. Ineffective porosity is the ratio of the closed pore volume to the total volume of the porous rock. Closed pores are ineffective in producing any reservoir fluid due to their total isolation, and are therefore of little interest in the study of hydrocarbon reservoirs.

Oil recovery depends on the ability for the reservoir rock to store and transmit oil. Effective porosity represents the pore spaces that are occupied by recoverable oil, and is therefore of great interest in terms of reservoir calculations. The effective porosity gives an indication of the reservoir rock potential to store accessible hydrocarbons. [9], [17], [14], [18], [20]

Equation 3-2 shows that the more porous reservoir rock, the higher volume of interconnected pores. Hence the greater capacity of the reservoir rock to store fluids. Important variables that influence the reservoir porosity are sorting of grains, grain shape, packing arrangement and degree of cementation. [3], [22]

3.2.1 Sorting of grains

Sorting describes the grain size uniformity of a reservoir rock. Well-sorted sediments have uniform grain size distribution, while poorly sorted sediments have a wide range in grain size distribution. [20] Figure 3-6 illustrates the difference between a well-sorted and a poorly sorted reservoir rock.

Figure 3-6: Sorting of grains. [23]

Well-sorted sediments give highly porous reservoirs. Since the grains are more or less equal, they leave large voids when they are packed. On the other hand, poorly sorted sediments result in lower porosity because the rock contains both larger and smaller grains that are out of proportion to each other. In rock formations, the smaller grains tend to fill in the voids in between the larger grains making it difficult for the oil to flow through the rock.

3.2.2 Grain shape

In sedimentary rocks, the grains come in varying size and shape. The sorting and packing arrangement of the grains will depend upon the fabric of the grains, such as roundness and sphericity. During the deposition and sedimentation, the edges of sharp mineral grains are polished. These processes round the sediments and make the grains more spherical. Roundness is not the same as sphericity. As the original shape of the grains controls the sphericity, the roundness is related to the roughness of the grains. [3] Figure 3-7 shows that mineral grains can be very angular but still have high sphericity

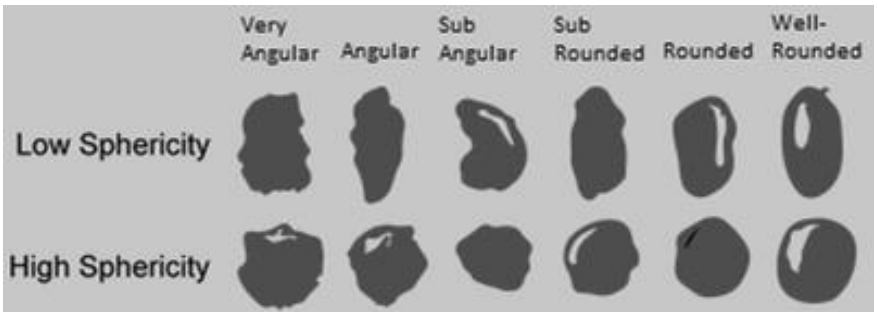

Figure 3-7: Varying roundness and sphericity of the mineral grains. [23]

Angular grains are compacted to fit together, causing low porosity. Well rounded grains, when packed together, have lots of voids in between the grains. This give an increase in the porosity of the rock and improve the ability to store larger volumes of oil. [3]

3.2.3 Packing arrangement of grains

The packing arrangement of grains refers to the structural organization of the mineral grains. The packing arrangement strongly affects the porosity of the rock. If well-rounded grains are packed into a cube, and the rock porosity varies from 26 % to 48 % depending on how the spheres are organized. [20] Figure 3-8 shows a system of well-rounded sediments of uniform size, packed in two different ways.

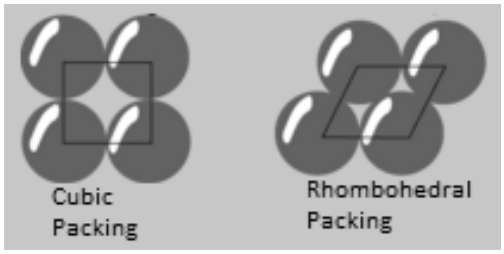

Figure 3-8: Cubic and rhombohedral packing of spheres. [23]

The most porous packing arrangement is the cubic packing, which ideally gives a porosity of approximately 48 %. The more cubic arrangement of spheres, the easier and more effective the oil is drained out. The most compact packing arrangement is ideal rhombohedral packing, with no more than 26 % porosity. In most sediments the spheres neither have uniform size nor are packed in an ideal structure, thus most sediments have much less than 48 % porosity, and commonly less than 26 % porosity. [20]

3.2.4 Degree of cementation

Porosity is classified either primary or secondary. In primary porosity the voids are formed at the time the sediments are deposited, while secondary porosity forms the voids after the deposition.

After deposition, processes of compaction and cementation change the fragments into sedimentary rocks, see Figure 3-9. Compaction refers to the pressing down of layers, forcing the sediment to fit closer together. Cementation refers to the process where new minerals crystallize and glue the sediment grains together. [22], [20]

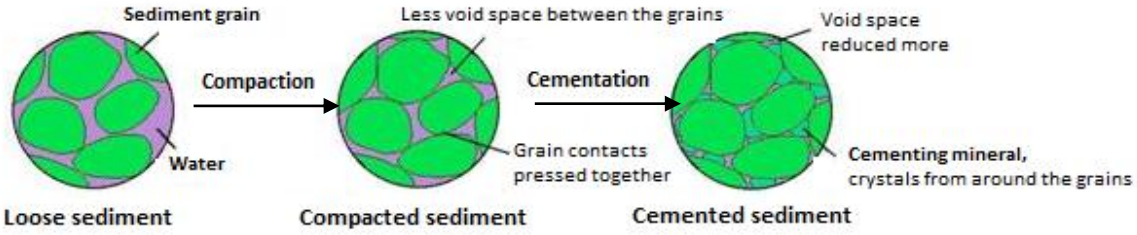

Figure 3-9: Compaction and cementation of sediments. [24]

Rocks with high degree of cementation might have pores completely isolated or disconnected from other pores. Thus heavy cementation reduces the porosity, and generally makes poor hydrocarbon reservoirs. [22], [20]

3.3 Saturation

The voids within a hydrocarbon reservoir are always completely filled with fluids. However, hydrocarbon fluids do not occupy all the available pores. As the sediment deposits, the pores are saturated with formation water. During compaction and cementation processes, hydrocarbons might enter the pores and force the formation water out. Still, a certain amount of the residual formation water will not be displaced and is always present in the reservoir. Oil, gas and water fills each a fraction of the total reservoir pore volume (V_{total}):

$$V_{total} = V_{oil} + V_{gas} + V_{water} \qquad [3\text{-}3]$$

The relative volume of each fluid presented in the pores is termed fluid saturation. Fluid saturation is expressed as the ratio of pore volume occupied by oil, gas or water to the total reservoir pore volume. This gives following equation for the oil saturation (S_{oil}):

$$S_{oil} = \frac{Volume\ of\ oil\ in\ the\ reservoir\ rock}{Total\ pore\ volume\ of\ the\ rock} \qquad [3\text{-}4]$$

Similar expressions can be written for the water saturation (S_{water}) and the gas saturation (S_{gas}). At any time the following relationship must hold true:

$$S_{oil} + S_{gas} + S_{water} = 1 \qquad [3\text{-}5]$$

The fluid saturation ranges from zero to nearly 100%. The oil saturation is always zero in a gas reservoir. And the gas saturation is zero in an oil reservoirs, as long as the reservoir pressure is above the bubble-point. As water is presented in all reservoirs, the water saturation is always greater than zero. [9], [17], [14], [25]

Saturation is a direct measure of the fluids in a reservoir rock, hence it directly influences the storage capacity of the reservoir. During oil extraction from an oil reservoir, oil saturation is reduced to a minimum saturation at which no more oil can escape from the pores. This occurs when the oil becomes immobile at the residual oil saturation (S_{or}). The corresponding endpoint saturation to water is the irreducible water saturation (S_{wc}) S_{wc} and S_{or} is further explained in Chapter 3.6.

The endpoint saturation for a reservoir fluid defines the saturation level below which the fluid cannot flow freely. The restrictions are due to forces between fluid-rock and fluid-fluid. The endpoint saturation for a specific fluid phase depends on the structure of the porous material along with the wettability and the extent of the displacement process that occurs. [25], [21] [26]

3.4 Wettability

Wettability is the most important factor influencing the ability for a particular fluid to flow within a porous rock. Wettability describes the preference for a reservoir rock to be in contact with one certain fluid phase, and it has a significant impact on the amount of and the distribution of the residual oil. [26] Hydrocarbon reservoirs can be either water-wet or oil-wet, depending on the tendency for one fluid over another, to spread or adhere to a solid surface. [27], [14] Figure 3-10 illustrates the difference between a water-wet and an oil-wet reservoir rock.

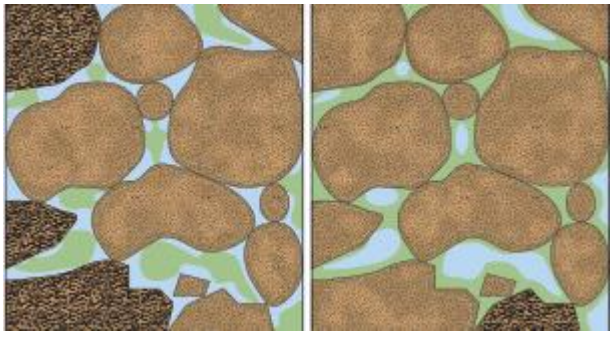

Figure 3-10: Wetting in pores. [28]

The water-wet reservoir has higher affinity for the water phase than for the oil phase. Water will occupy the smaller pores and will preferably stick to the grain surface in the larger pores. In water-wet reservoirs, with high oil saturation, attractive forces between the rock and the fluid draw the water into the smaller pores- While repulsive forces cause the oil to remain in the center of the largest pores. The opposite condition is oil-wet reservoir, in which the pore surface prefers contact with the oil phase and oil absorbs into the smaller pores. The wetting phase fluid often has low mobility, while the non-wetting fluid is more mobile and especially at large non-wetting phase saturations.

Wettability depends on the surface roughness and varies with grain shape, grain size and roundness. Wettability in a hydrocarbon reservoir is determined by a combination of all the surface forces acting, when two immiscible fluids are in contact with a solid. [9], [28], [25]

3.4.1 Interfacial tension

Oil and water are usually immiscible. But, when they co-exist within a reservoir rock interactions cause changes in the spatial distributions and movements. This is due to forces acting between the fluids, causing a thin film or a clear interface to develop at the boundary between the fluid surfaces. The forces exerted by the fluid interfaces are dissimilar, leading to interfacial tension. Interfacial tension is the measure of the force that holds the surfaces of two immiscible fluids together. [26] The equation that describes the balance of forces acting in an oil-water system is:

$$\sigma_{ow} \cdot cos\theta = \sigma_{os} - \sigma_{ws} \qquad [3\text{-}6]$$

Where σ_{ow} is the interfacial tension that occurs between the oil phase and the water phase. σ_{os} is the interfacial tension between the oil phase and the pore surface and σ_{ws} is the interfacial tension between the water phase and the pore surface. Theta (θ) is the observed contact angle between the pore surface and the slope of the droplet.

Interfacial tension results in resisting miscibility between the fluid phases, and might cause a certain resistance in the fluid flows within the reservoir. [26] Figure 3-11 illustrates the relationship between interfacial tension and wettability for a water-wet and an oil-wet reservoir rock.

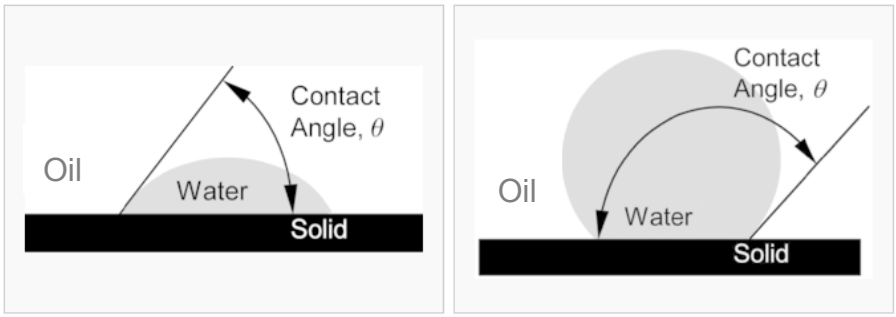

Figure 3-11: Wettability in a reservoir rock. [4]

Wettability is determined by the contact angle between the three phases. A common rule of thumb is that the reservoir rock is water-wet if θ is below 80°, and oil-wet if θ is larger than 100°. If θ is between 75° and 105° the reservoir rock is intermediate-wet, in which oil and water have the same tendency to spread to the pore surface. [36], [25], [9], [26]

3.4.2 Capillary Pressure

Capillary pressure is an important parameter when studying a hydrocarbon reservoirs. Along with the viscous and the gravitational forces, the capillary forces control the fluid

distributions and the fluid flows within the reservoir rock. The existence of capillary pressure is the result of interfacial tension between the rock and the fluids, and between two immiscible fluid phases. [4]

Capillary pressure is related to the capillary phenomena that occurs when two immiscible fluid phases are in contact with each other in a capillary-like tube. The connected pores in a reservoir can be considered as capillary tubes with very low diameter. When two immiscible fluid phases are in contact inside a porous rock, the interfacial tension between the wetting phase and the rock is greater than that between the non-wetting phase and the rock. The wetting phase will move along the pore surface while the non-wetting phase will be trapped in the center. [9],[28],[29], [6] Figure 3-12 shows an illustration of the capillary phenomenon in a tube.

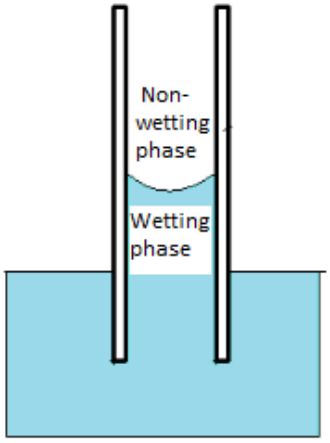

Figure 3-12: Capillary pressure in a tube.

The capillary pressure (P_c) is defined as the molecular pressure difference measured across the interface between two immiscible fluids, the mathematically expression is:

$$P_c = P_{nw} - P_w \qquad [3\text{-}7]$$

Where P_{nw} and P_w refer to the pressure from the non-wetting fluid and the wetting fluid respectively. The pressure exerted by the non-wetting fluid is higher than that exerted by the wetting fluid, causing the curvature of the interface to be convex into the wetting fluid. [29]

By implementing the Young-Laplace equation (Equation 3-8), the curves that form the meniscus can be used to calculate the capillary pressure for the immiscible fluids, see Figure 3-13. [30]

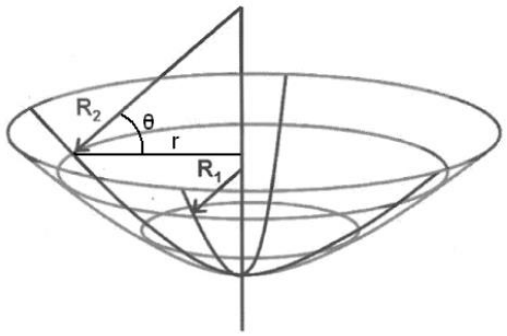

Figure 3-13: The interface between two immiscible fluids. [30]

The Young-Laplace equation is expressed as:

$$P_c = \sigma_{nw}(\frac{1}{R_1} + \frac{1}{R_2}) \qquad [3\text{-}8]$$

$R_1$and R_2 describes the radius of the curves and σ_{nw} is the interfacial tension between the non-wetting phase and the wetting phase. From the geometry it is known that:

$$R_2 = \frac{r}{cos\theta} \qquad [3\text{-}9]$$

Assuming the meniscus is circular so that $R_1 = R_2$, the capillary pressure can be expressed in terms of the pore radius and the interfacial tension: [30] [6]

$$P_c = \frac{2 \cdot \sigma_{nw} \cdot cos\theta}{r} \qquad [3\text{-}10]$$

r is the pore radius and θ is the contact angle. From Equation 3-10 it is seen that the capillary pressure is proportional to the interfacial tension, and inversely proportional to the radius. The smaller pore radius, the further the wetting phase moves into the pore channel and the higher capillary pressure. [18] [28] [6] Figure 3-14 shows how the capillary pressure curve is controlled by the pore size distribution.

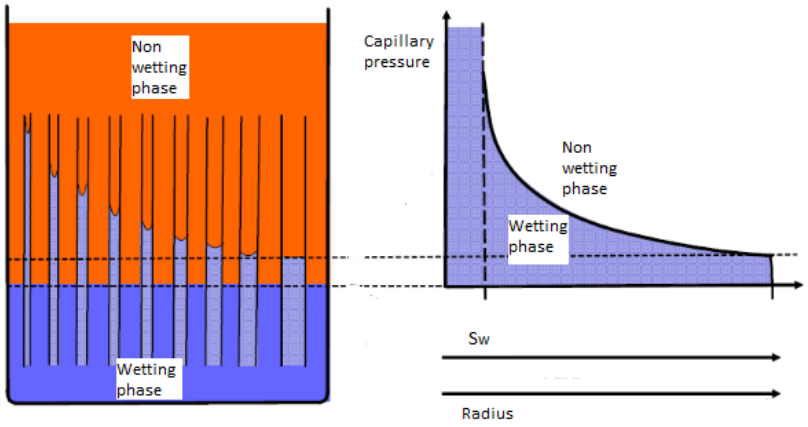

Figure 3-14: Capillary tubes of different sizes and the relationship between the pore size distribution and the capillary pressure curve. [30]

The capillary pressure causes the interface to rise inside the capillary tubes until the buoyancy forces balance the capillary forces. The capillary forces are associated with the capillary pressure. Thus small radius gives high capillary pressure, as the height of water increases with decreasing capillary tube radius. [30] The shape of a capillary pressure curve is therefore closely related to the pore size distribution:

$$P_c = \Delta\rho g h \qquad [3\text{-}11]$$

There are two types of capillary pressure processes; drainage and imbibition. In a drainage process, the non-wetting phase displaces the wetting phase. The reverse process is imbibition, where the wetting phase displaces the non-wetting phase. To generate a drainage capillary pressure curve, the wetting phase saturation is reduced from maximum to minimum by increasing the capillary pressure from zero to a large positive value. [4]

3.5 Permeability

Permeability is the measure of how easily a porous rock will allow passage of fluids. Permeability is a dynamic property, meaning it varies within the reservoir depending on flow direction and position. Figure 3-15 shows the fluid flow within a reservoir rock. The fluids can easily flow within interconnected pores, but cannot enter a closed pore.

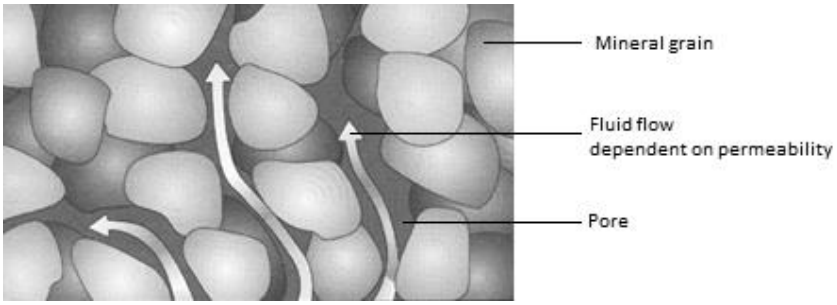

Figure 3-15: Relation between fluid flow and rock permeability. [32]

The fundamental physical law that governs the rock permeability is complex. For the purposes of fluid flows in a rock, it is convenient to assume laminar flow. This assumption allows great simplification of the flow equation, leading to Darcy's law:

$$Q = A\frac{K}{\mu}\cdot\frac{dp}{dx} \qquad [3\text{-}12]$$

Where K is the rock absolute permeability of the fluid phase, Q represents the volumetric flow rate of the fluid through the cross-sectional area A, μ is the fluid viscosity and $\frac{dp}{dx}$ is the flow potential drop for the fluid over the flow length *x*. [21], [14], [34], [31], [17]

Absolute permeability defines the permeability when the voids are saturated with one single fluid phase. The permeability of a single fluid is different to the permeability of the fluid when more than one fluid phase flows within the porous rock. In a reservoir rock where more than one fluid flow, effective and relative permeability is introduced. Such multi-phase flow is common in most of the hydrocarbon reservoirs. In multi-phase systems it is necessary to quantify the fluid flow for each of the fluid phases in the presence of the other fluid phases. The flow calculation is a modification of Darcy's law:

$$Q_i = A\frac{K_i}{\mu_i}\cdot\frac{dp_i}{dx} \qquad [3\text{-}13]$$

Where *i* refers to each of the specific fluid phases. [21], [9]

In hydrocarbon reservoirs, two and sometimes three phases generally are present, i.e. oil, gas and water. The effective permeability to either fluid is expected to be lower than that for the single fluid. This is because the fluid occupies only parts of the voids and may be affected by interactions with the other phases. In multi-phase systems, it is usual to express permeability as relative permeability.

3.5.1 Relative permeability

The relative permeability is defined as the ratio of the effective permeability (K_i) to the absolute permeability (K):

$$K_{ri} = \frac{K_i}{K} \qquad [3\text{-}14]$$

K_{ri} refers to relative permeability of the specific fluid phase *i*, hence relative permeability of oil, gas and water in a reservoir rock is denoted K_{ro} , K_{rg} and K_{rw} respectively.

[17], [14], [18]

Relative permeability is a function of various physical properties, including pore-geometry, rock wetting characteristic, fluid saturation and reservoir temperature and pressure. [21] Relative permeability is often displayed in diagrams, plotted as a function of the fluid saturations. Figure 3-16 and Figure 3-17 present typical relative permeability curves for oil and water in a water-wet and an oil-wet reservoir rock respectively. The irreducible water saturation (S_{wc}) defines the maximum water saturation that a reservoir can retain without producing water. This water is held in place by capillary forces and will not flow. (S_{or}) refers to the residual oil saturation, at which oil no longer can be recovered by primary and secondary oil recovery, only by enhanced oil recovery. K_{rowc} is the relative permeability of oil at the irreducible water saturation and K_{rwoc} is the relative permeability of water at the residual oil saturation. [25], [27], [14], [18]

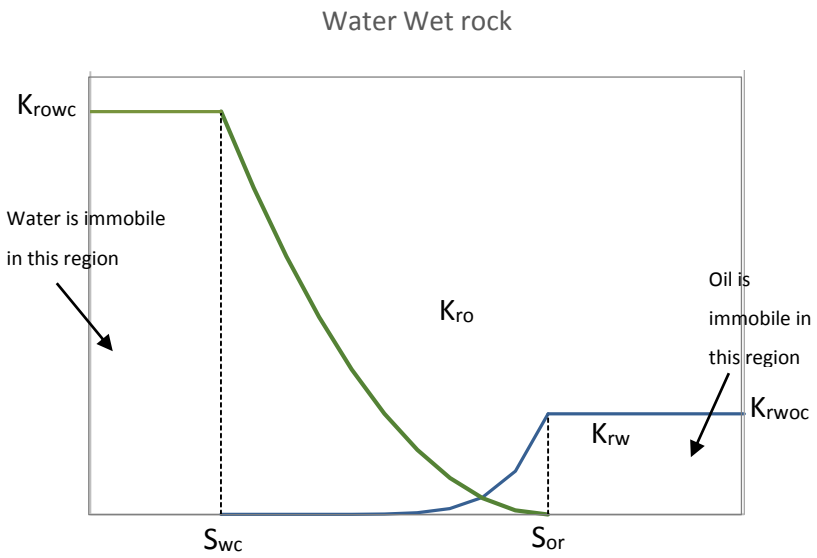

Figure 3-16: A schematic of oil-water relative permeability curves in water-wet rock.

In a water-wet system, the wetting phase is water. Initially, at S_{wc} water will not be capable to flow. Relative permeability of water (K_{rw}) is zero and relative permeability of oil (K_{ro}) is K_{rowc}. As water is flooded into the reservoir, the water saturation (S_w) increases. Water migrates, tending to displace most of the oil in the pores. The oil flow ceases abruptly and K_{ro} decreases until it effectively reaches zero at some high water saturation corresponding to S_{or}. [27] [34] Water-wet reservoirs are usually described by restricted movement of water and low K_{rwoc}. Water-wet reservoirs generally give good oil recoveries, but oil production after water breakthrough is limited.

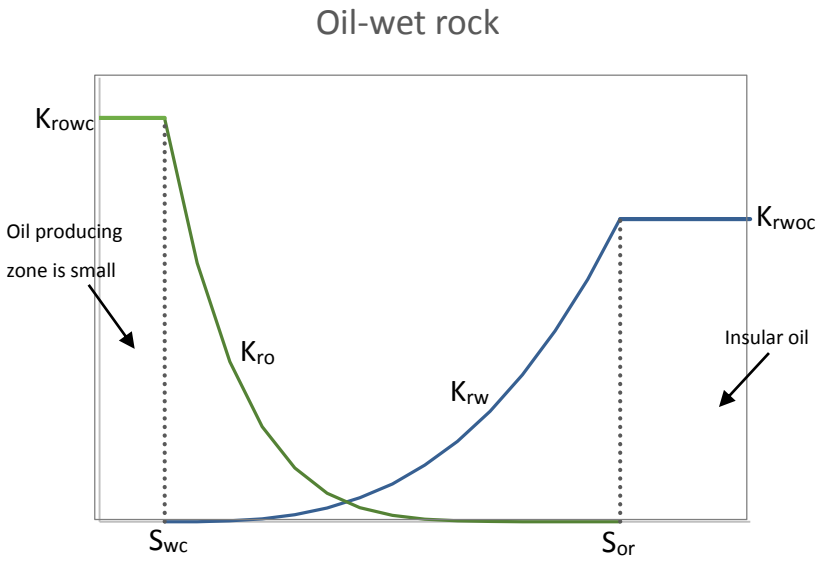

Figure 3-17: A schematic of oil-water relative permeability curves in oil wet rock.

When water is flooded into an oil-wet pore system, the water flows through the largest pores first. This causes an earlier breakthrough of water. K_{ro} decreases rapidly as K_{rw} increases slightly. After large volumes of water have flown through the reservoir, S_{or} is reached. [34] Oil-wet reservoirs are characterized by low S_{wc} and high S_{or}. K_{ro} is always less than K_{rw} at a given S_w in an oil-wet reservoir compared to a water-wet reservoir.

The plots in Figure 3-16 and Figure 3-17 show that the wettability has significant impact on the relative permeability curves. Hence the wettability affects the potential for oil production from the reservoir. The relative permeability in a water-wet reservoir differs from the relative permeability in a water-wet reservoir because of the difference in the fluid distributions. Table 3-1 presents some general rule of thumbs in characterizing a water-wet and an oil-wet reservoir.

Table 3-1: Relative permeability characteristics in water-wet and oil-wet reservoirs. [4]

	Oil-wet	**Water-wet**
Irreducible water saturation (S_{wc})	Generally less than 15 %, frequently less than 10 %	Usually greater than 20 %
Saturation at which oil and water relative permeability are equal ($K_{rw} = K_{ro}$)	Less than 50 % water saturation	Greater than 50 % water saturation
Relative permeability to water at maximum water saturation (K_{rwoc})	Greater than 50 %, and approaching 100 %	Generally less than 30 %

3.5.2 Relation between porosity and permeability of a reservoir rock

Permeability depends upon porosity, the higher porosity the higher permeability. However, permeability also depends upon the type of pores. In addition to being porous, a reservoir rock must have the ability to transmit fluids through interconnected pores. A rock may have high porosity, but still have no fluid conductivity for lack of pore interconnections. If the fluids occupy the unconnected voids within a reservoir, they cannot be produced. [34] Figure 3-18 illustrates the relationship between porosity and permeability.

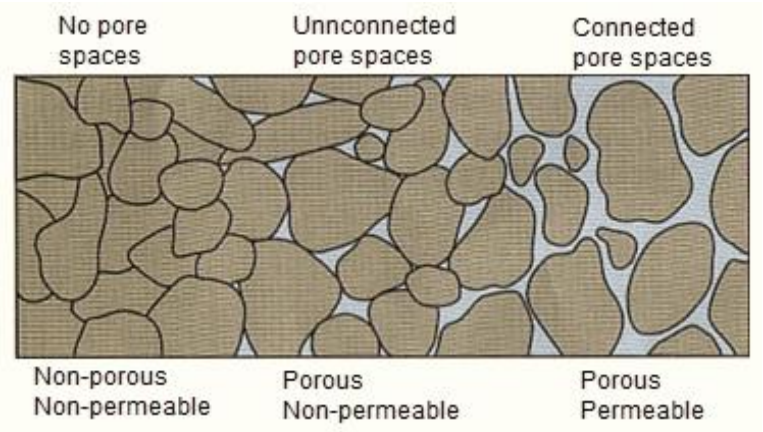

Figure 3-18: Relationship between porosity and permeability. [33]

Various properties of the grains, including grain size and grain size distribution affects how the pores are connected. From Figure 3-18 it is seen that low porosity results in low permeability, but high porosity does not necessarily indicate high permeability. Smaller

grain size means more restricted fluid flow, thus lower permeability. This is due to the smaller grains producing smaller pores and smaller pore channels, which causes larger friction between the fluid and the rock. [34]

4 Carbonate reservoirs

More than 60 % of the world's oil resources occur in carbonated rocks [6]. Although carbonate reservoirs contain a majority of the oil reserves, only small amounts of the production worldwide come from these reservoirs [6] Generally, carbonate reservoirs have complicated pore structures and strong heterogeneity. The heterogeneity in carbonates is one of the main reasons causing low oil recovery from these reservoirs. Carbonate reservoir rocks heterogeneity is the result of a complex mineral composition and a complex rock texture. Carbonate reservoirs are characterized by highly variability in their petrophysical properties within small sections of the reservoir [6], [35]

4.1 Petro physical properties of carbonate reservoirs

Porosity and permeability are the most important factors when the reservoir quality is described. The original grain shape and grain size distribution control the porosity, but porosity is also a result of the secondary processes involving compaction and cementation of the sediments. Porosity in carbonate reservoirs vary from 1 % - 37 %. [6]

In carbonate reservoirs, the porosity and the permeability are controlled by the presence and the distribution of open fractures. Most carbonate reservoirs are naturally fractured. Fractures are high permeability pathways for hydrocarbon migration in a low permeability rock. Fractured corridors exist in all scales, ranging from microscopic cracks to fractures of ten to hundreds of meters in width and height. [35] [6] Permeability varies greatly in carbonate reservoirs, from values less than 0.1 mD in cemented carbonates to over 10 000 mD in fractures [6]

A great majority of carbonate reservoirs tend to be oil-wet. Extensive research work on wettability for carbonate reservoir rocks confirms that carbonates exhibit significantly more oil-wet character than water-wet character. Performed contact angle measurements show that 15 % of carbonates are strongly oil-wet (θ=160°-180°), 65 % are oil-wet (θ=100°-160°), 12 % are intermediate-wet and 8% are water-wet. [36] Evaluations of wettability for the carbonate rock samples, using relative permeability curves and Amott tests conclude that the carbonate reservoirs investigated ranges from intermediate-wet to oil-wet. [36]
Presumed petrophysical properties of carbonate reservoirs are presented in Table 4-1.

Table 4-1: Petro physical properties of carbonate reservoirs. [6], [35]

	Porosity	**Permeability**	**Permeability in fracture**	**Wettability**
Range	0.01 -0.3	0.7-130 mD	Large	Intermediate-wet to strongly oil-wet

5 Simulation of oil production and CO_2 distribution in carbonate reservoir

The near-well simulations of CO_2-injection and CO_2 distribution in carbonate reservoirs, were carried out using the commercial reservoir simulation software Rocx, in combination with OLGA. The OLGA software is the main program, but several additional modules are developed to solve specific cases.

5.1 Simulation software OLGA/Rocx

Criterion for the performed simulations was a carbonate reservoir with fracture. The geometry for the simulated carbonate reservoir is 105 m in length, 96 m in width and 50 m in height. 3 grid blocks are defined in *x*-direction, 25 in *y*-direction and 10 in *z*-direction. The well is located 35 m from the bottom, and indicated as a black dot in Figure 5-1. The radius of the wellbore is 0.15 m, Figure 5-1 shows the grid and geometry of the simulated reservoir section at initial conditions.

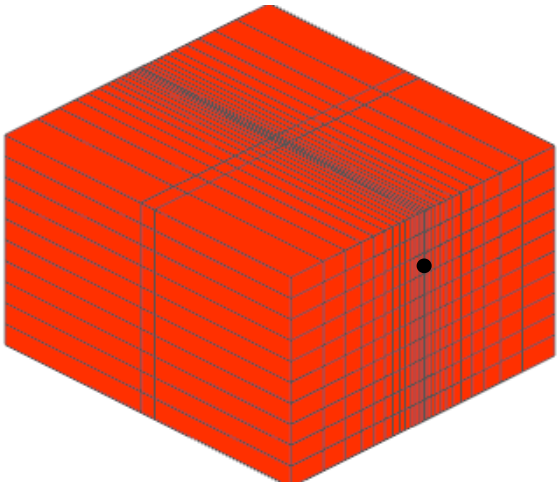

Figure 5-1: Grid and geometry of the simulated reservoir.

The reservoir is divided into three zones in *x*-direction. A constant porosity of 0.15 is used in the entire reservoir. A permeability of 4000 mD is set in the second zone, and a permeability of 40 mD is set in the first and the third zone. The second zone represents the fractured part, thus the permeability is set much higher in this zone compared to the two other zones. The temperature is maintained constant at 76°C and the waterdrive pressure from the bottom of the reservoir is 176 bar, the wellbore pressure is set to 130 bar. The reservoir and fluid properties for the simulations carried out are presented in Table 5-1.

Table 5-1: Reservoir and fluid properties for the specific simulations.

Properties	**Value**
Oil viscosity	10 cP
Reservoir pressure	176 bar
Reservoir temperature	76°C
Oil specific gravity	0.8
Porosity	0.15
Permeability first zone (*x- y-z- direction)*	40-40-20 mD
Permeability second zone (in *x-y-z-direction)*	4000-4000-2000 mD
Permeability third zone (in *x-y-z-direction)*	40-40-20 mD
Wellbore pressure	130 bar

The simulation software Rocx generates the relative permeability curves. The calculations are based on the Corey correlation, a power law relationship with respect to water saturation. These calculations are shown in Chapter 5.2.1.

The module Rocx is connected to OLGA by the near-well source component in OLGA, which allows importing the file created by Rocx. In order to get a simulation of the complex system including valves and packers, OLGA requires both a "Flowpath" and a "Pipeline" as shown in Figure 5-2.

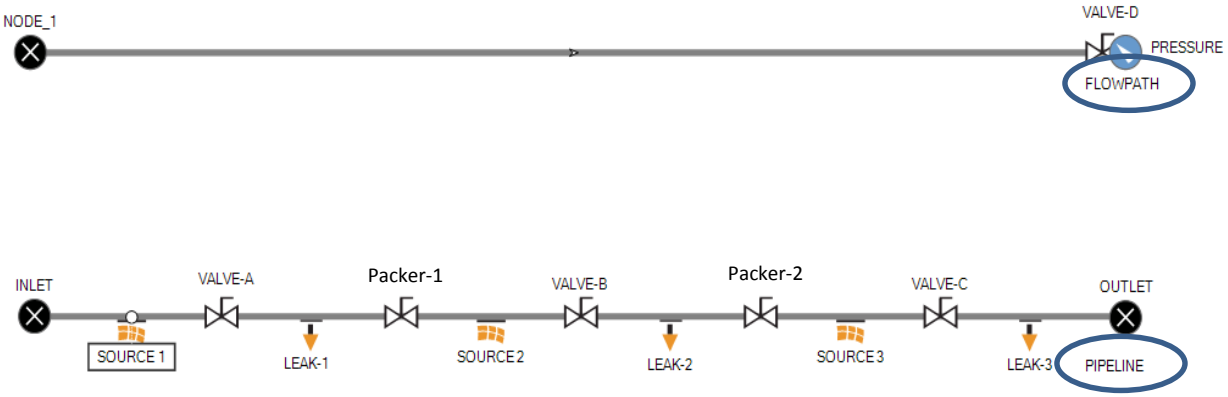

Figure 5-2: OLGA study case for the performed simulations.

In the simulations the “Flowpath” represents the pipe and the “Pipeline” represents the annulus. The annulus is the space between the pipe and the rock, see Figure 5-3. [28]

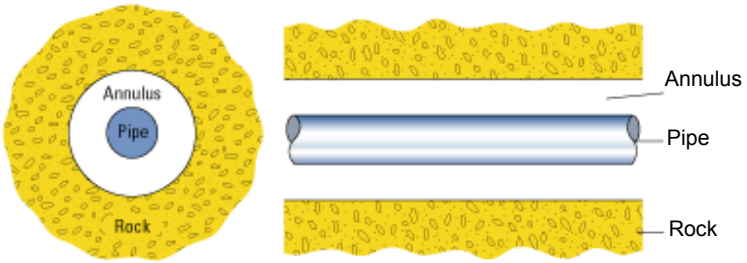

Figure 5-3: A schematic of the pipe and the annulus. [28]

As seen from Figure 5-4 the “Flowpath” is divided into six equal sections. The sources implemented in the “Pipeline” are connected to the boundaries in Rocx, and indicate the inflow from the reservoir into the annulus. The leaks indicate the inflow from the annulus into the pipe, through the control valves A, B and C. The packers are simulated as closed valves and are installed to isolate the different production zones in the well.

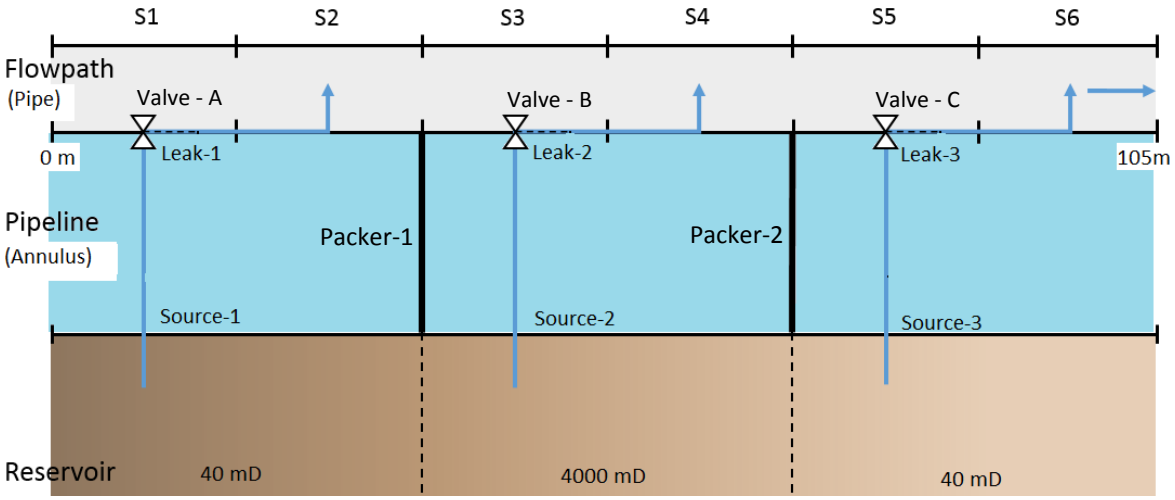

Figure 5-4: The near-well simulation in OLGA. [5]

In the simulations the packers divide the “Pipeline” into three zones. The inflow from Source-1 goes from section one in the annulus and enters the pipe in section two. Similarly for the flow in production zone two and three.

5.2 Simulation cases

The simulations are carried out for an oil-wet carbonate reservoir with fractures. To solve the problem with high production rate in the fractured zone, the control valve in this zone (Valve-B) is closed in Case 3 and Case 4. The detailed specifications for the six different cases that are simulate are listed in Table 5-2.

Table 5-2: Simulation cases.

Case 1	**Case 2**	**Case 3**	**Case 4**	**Base Case 1**	**Base Case 2**
With Fracture	With Fracture	With Fracture	With Fracture	Without Fracture	Without Fracture
Without CO_2-injection	With CO_2-injection	Without CO_2-injection	With CO_2-injection	Without CO_2-injection	With CO_2-injection
Valve-B Open	Valve-B Open	Valve-B Closed	Valve-B Closed	Valve-B Open	Valve-B Open

5.2.1 Relative permeability curves

The relative permeability curves for oil and water used in the simulations are generated using Corey's model. The model is derived from capillary pressure data and is widely accepted as a good approximation for relative permeability curves in a two-phase flow. The required input data is limited to the end-points S_{wc} and S_{or}, and their corresponding relative permeability. [37]

$$K_{rw} = K_{rwoc}\left(\frac{S_w - S_{wc}}{1 - S_{wc} - S_{or}}\right)^{n_w} \quad [5\text{-}1]$$

$$K_{ro} = K_{rowc}\left(\frac{1 - S_w - S_{or}}{1 - S_{wc} - S_{or}}\right)^{n_{ow}} \quad [5\text{-}2]$$

n_w and n_{ow} are the Corey coefficients for water and oil respectively. The coefficients are functions of the pore size distribution in the reservoir and are therefore reservoir specific. K_{rwoc} and K_{rowc} constrain the relative permeability at the S_{wc} and the S_{or}. The relative permeability between the end-points is controlled by n_w and n_{ow}. The Corey coefficients strongly influence the relative permeability curves, as the relative permeability changes when the pore-geometry change. Typical values for the Corey coefficient for an oil-wet reservoir are shown in Table 5-3. [37]

Table 5-3: Corey coefficient in oil-wet reservoirs. [37]

Corey coefficient	**Value**
$\mathbf{n_w}$	2-3
$\mathbf{n_{ow}}$	6-8

Figure 5-5 shows the relative permeability curves plotted with different the values of the Corey's exponent, n_w and n_{ow}, for an oil-wet carbonate reservoir. The green lines represent the relative permeability of oil and the blue lines represent the relative permeability of water.

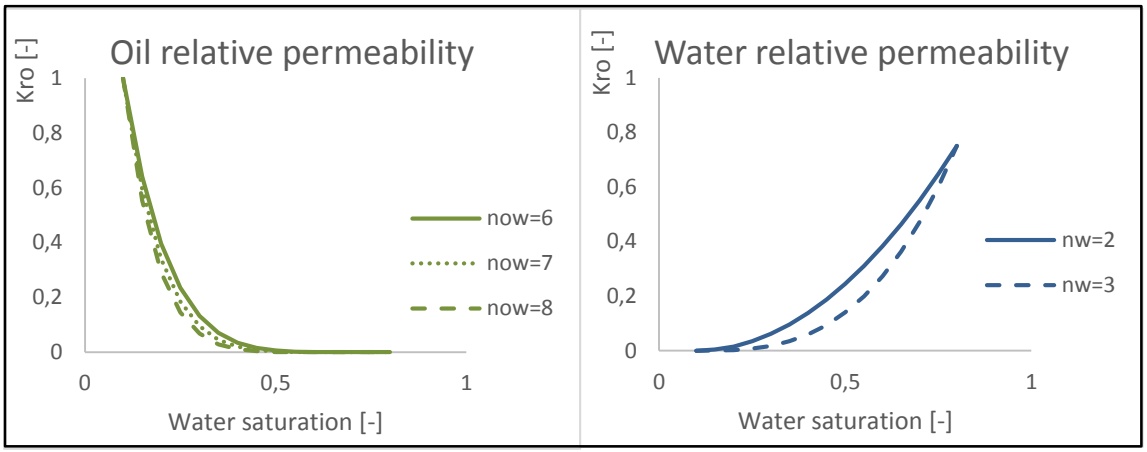

Figure 5-5: Oil and water relative permeability curves for an oil-wet reservoir, with variable values for the Corey coefficient.

The plots indicate that high Corey coefficient for the non-wetting phase results in a more concave relative permeability curve. This is as expected, because high Corey coefficient indicates more heterogeneous reservoir. Thus, lower relative permeability. Low Corey coefficient indicates high uniformity of pores and a more homogeneous reservoir, resulting in higher relative permeability and less concave permeability curve. [13]

In addition to the six cases described in Table 5-2, two cases were simulated for a water-wet carbonate reservoir with fractures. The specifications and the results from these simulations are presented in Appendix C.

To simulate CO_2-injection into the reservoir, it was necessary to correlate for the effects of CO_2 to the relative permeability curves. The correlation resulted in new Corey's exponents and new residual oil saturations used to generate the new relative permeability curves. CO_2-injection reduces the interfacial tension and the oil viscosity, and causes oil swelling. Based on these parameters, the following relations was implemented to calculate the Corey's exponents and the residual oil saturation for simulation with CO_2-injection: [13], [37]

$$n_{ow}(CO_2 - injection) = 0.568951 \cdot n_{ow} \quad [5\text{-}3]$$

$$S_{or}(CO_2 - injection) = 0.754288 \cdot S_{or} \quad [5\text{-}4]$$

The definition and the explanation of the correlation factor used to derive the expressions in Equation 5-3 and 5-4 are found in Appendix D.

The relative permeability curves for the performed simulations are generated in Rocx, using the data listed in Table 5-4.

Table 5-4: Relative permeability data for the specific simulation cases.

	S_{wc}	S_{or}	K_{rowc}	K_{rwoc}	n_w	n_{ow}
Base Case 1, Case 1 and Case 3	0.1	0.2	1	0,75	3	6
Base Case 2, Case 2 and Case 4	0.1	0.1	1	0,75	3	3,4

For the simulations without CO_2-injection (Base Case 1, Case 1 and Case 3) the Corey's coefficients n_w and n_{ow} are set to 3 and 6 respectively. The residual oil saturation (S_{or}) is 0.2.

For the cases with CO_2-injection into the reservoir (Base Case 2, Case 2 and Case 4) n_{ow} is reduced to 3.4 and S_{or} is reduced to 0.1. These values are calculated according to Equation [5-3] and [5-4]. n_w , S_{wc} , K_{rowc} and K_{rwoc} are equal for all simulation cases.

Figure 5-6 shows the implemented relative permeability curves for the specific cases. The green lines represent the relative permeability of oil (K_{ro}) and the blue lines represent the relative permeability of water (K_{rw}). The cases without CO_2-injection are indicated by solid lines and the cases with CO_2-injection into the reservoir are indicated by dotted lines.

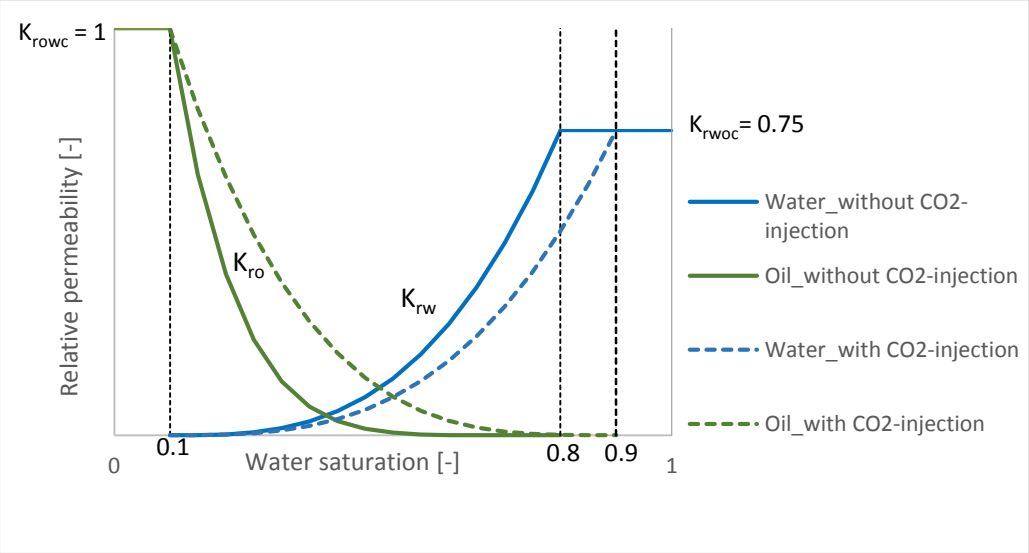

Figure 5-6: Relative permeability curves in oil-wet reservoir.

Initially, when the water saturation is equal to the critical water saturation ($S_w = S_{wc}$) the injected CO_2 does not contact fully with the oil, and the difference in K_{ro} between the two cases is low. As oil saturation decreases, the movement of oil becomes more difficult and the injected CO_2 will improve the oil flow by lowering interfacial tension and the oil viscosity. The CO_2-injection may lead to reduced trapped oil and lower reduced residual oil saturation by swelling mechanism. This results in higher relative permeability for oil, especially in the low oil saturations.

5.2.2 Input to OLGA and Rocx

All six cases include the reservoir and the fluid properties listed in Table 5-1, page 38. The input to Rocx and OLGA for each case is listed in Table 5-5.

Table 5-5: Input for the performed simulations.

Simulation Case	Data input to Rocx	Relative permeability curve	CO_2-injection	Position Valve A and Valve C	Position Valve B
Base Case 1	See Table 5-1*	See Figure 5-6	No	Open	Open
Base Case 2	See Table 5-1*	See Figure 5-6	Yes	Open	Open
Case 1	See Table 5-1	See Figure 5-6	No	Open	Open
Case 2	See Table 5-1	See Figure 5-6	Yes	Open	Open
Case 3	See Table 5-1	See Figure 5-6	No	Open	Closed
Case 4	See Table 5-1	See Figure 5-6	Yes	Open	Closed

* The base cases are the simulations where the reservoir rock has no fractures, hence the permeability is set to 40 mD in all production zones.

Base Case 1, Case 1 and Case 3 are presented by the relative permeability curves indicated as a solid line in Figure 5-6. In Case 1 all control valves A, B and C are fully open during the simulation. In Case 3 the control valves located in the first and the third production zone (Valve A and Valve C) are open, while the control valve located in the second production zone (Valve B) is closed. In Base Case 2, Case 2 and Case 4 CO_2 is injected into the reservoir. Assuming that the oil and water relative permeability curves are significantly changed due to the CO_2-injection, new relative permeability curves are implemented. The relative permeability curves implemented for Base Case 2, Case 2 and Case 4 are seen as a dotted line in Figure 5-6. In Case 2 all the control valves A, B and C are fully open. In Case 4 the control valves A and C are open and the control valve B is closed. All simulations where run for 400 days.

6 Results

In this chapter the results from the simulations of oil production and CO_2-distribution in a carbonate reservoir are presented. Chapter 6.1 includes the results from the base case simulations. Chapter 6.2 presents the results from Case 1 and Case 2 and Chapter 6.3 presents the results from Case 3 and Case 4. In Chapter 6.4 the CO_2-distribution in the carbonated reservoir is studied.

6.1 Oil production from a homogenous carbonate reservoir

This subchapter focuses on the oil production and the affection of CO_2-injection into a homogeneous carbonate reservoir. Two different cases were simulated for the reservoir, Base Case 1 and Base Case 2. The base cases are the cases where the reservoir rock has no fractures, so that the permeability is set the same in all three production zones. The permeability is set to 40 mD, which is normal properties of carbonated sediments. Base Case 1 simulates water displacing the oil by waterflooding. Base Case 2 simulates injection of CO_2 into the reservoir, thus the CO_2 displaces the oil. Figure 6-1 shows the accumulated oil and water production from the reservoir under the specified conditions. The red lines represent Base Case 1, the green lines represent Base Case 2, the solid curves represent oil and the dotted curves represent water.

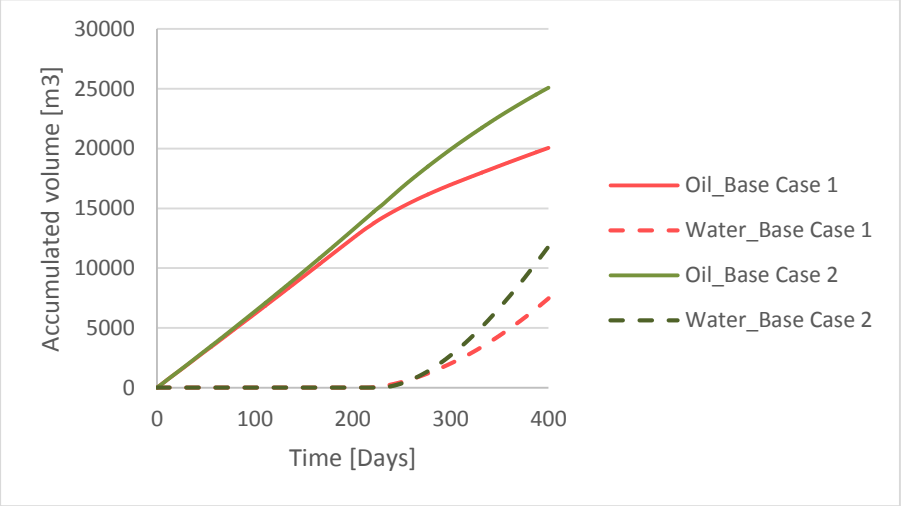

Figure 6-1: Accumulated oil and water, Base Case 1 and Base Case 2.

As seen from Figure 6-1 the accumulated oil volume is higher in Base Case 2 than in Base Case 1. Thus, CO_2-injection into the reservoir gives an increase in the oil production. Accumulated oil volume is increased by 5000 m^3, from 20000 m^3 oil in Base Case 1 to 25000

m^3 in Base Case 2. Simultaneously, the production of water is increased. The accumulated water volume increases with 4000 m^3 for Base Case 2 compared to Base Case 1, from 7500 m^3 water in Base Case 1 to 11500 m^3 in Base Case 2.

Immediately after flooding of water and CO_2, oil production is initiated from the reservoir. The accumulated oil volume is rising steadily for both cases. After 60 days the curves split, and the increase in accumulated oil volume in Base Case 1 is slowed as the production rate stabilizes. Base Case 2 continues to rise with a steeper slope until water breakthrough occurs for this case after 280 days. This is seen more clearly in Figure 6-2, where the volumetric flow rate of oil and water in Base Case 1 and Base Case 2 are displayed. The red lines represent Base Case 1, the green lines represent Base Case 2, the solid curves represent oil and the dotted curves represent water.

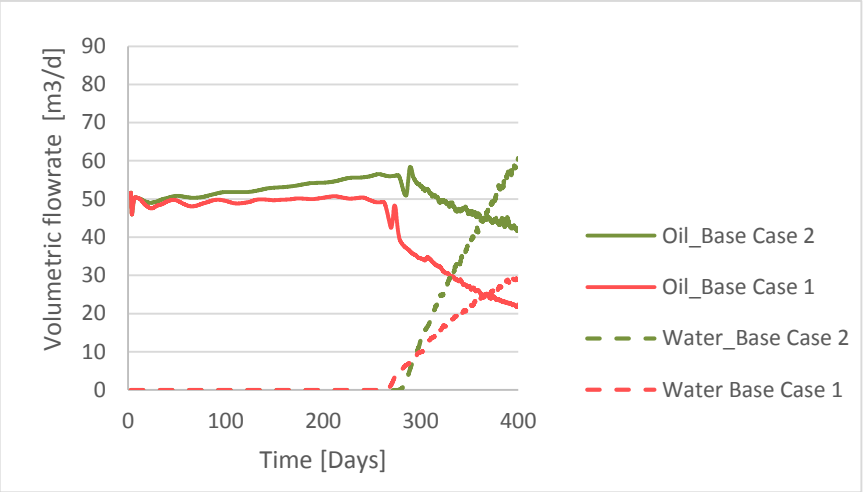

Figure 6-2: Volumetric flowrate of oil and water, Base Case 1 and Base Case 2.

The oil production rate for Base Case 1 remains more or less constant at 50 m^3/day for 260 days, at this time water breakthrough occurs and the well starts to produce water along with the oil. The oil production rate then decreases rapidly from 50 m^3/day to 22 m^3/day. For Base Case 2 the oil production rate increases slightly, from 50 m^3/day to nearly 60 m^3/day, until water breakthrough occurs after 280 days. Immediately after water breakthrough, the oil production rate slowly decreases to 44 m^3/day and the water production rate increases very rapidly to 60 m^3/day. Due to CO_2-injection into the reservoir, CO_2 comes with the produced water in Base Case 2 In Figure 6-3 the total liquid flowrate in the different sections in the pipe is seen. The total liquid flowrate includes the flowrate for both oil, water and CO_2. The plot displays Base Case 2.

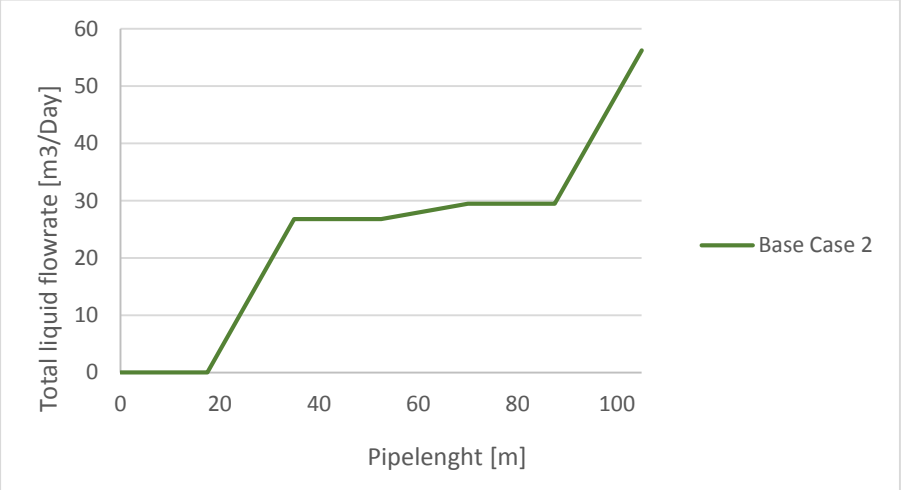

Figure 6-3: Total liquid volumetric flowrate in pipe, Base Case 2.

From Figure 6-3 is seen that the liquid flowrate increases along with the pipelenght. In section 1, 3 and 5 the liquid flowrate is constant, this is as expected since these are the sections where the fluid flows from the reservoir and into the annulus. There is no possibility for the liquid to enter the pipe in these sections. Section 2, 4 and 6 represent the three production zones where the flow goes from annulus and into the pipe, hence the liquid flowrate in the pipe increases in these sections. As seen, section 4 has low production rate due to more narrow production area.

6.2 Oil production from a carbonate reservoir with fracture

This subchapter focuses on the oil and water production from a heterogeneous carbonate reservoir with fracture. Two different cases were simulated for the reservoir, Case 1 and Case 2. The fracture in the reservoir is specified as a high permeability zone, thus the permeability in the second production zone is set significantly larger than the permeability in the other two zones. The permeability is set to 4000 mD in the second production zone and 40 mD in the first and third production zone. Figure 6-4 shows the accumulated oil and water volume for the two cases. Case 1 simulates water displacing oil by waterflooding and is colored orange in the diagram. Case 2 simulates injection of CO_2 into the reservoir and is colored purple. The solid lines represents oil and the dotted lines represent water.

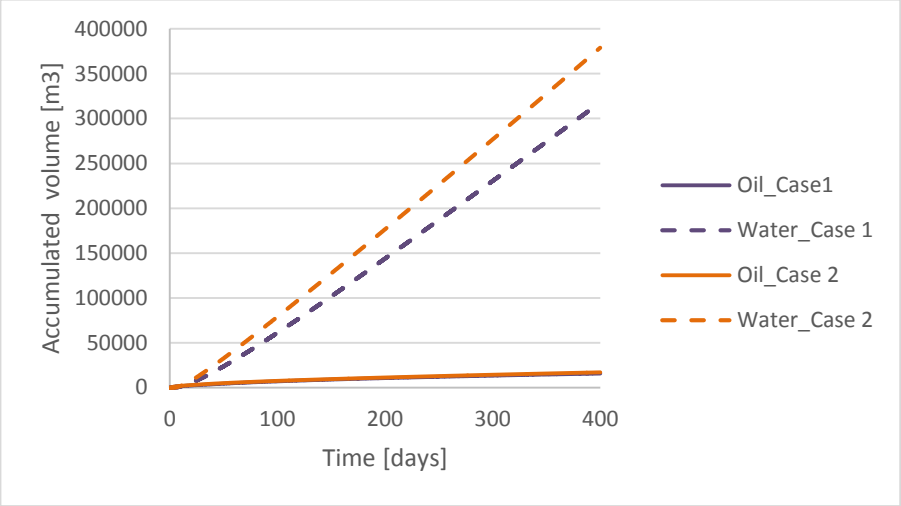

Figure 6-4: Accumulated oil and water, Case 1 and Case 2.

Initially, at the time water and CO_2 enter the reservoir, the oil production rate is very high. The curves for the accumulated oil volume in Case 1 and Case 2 follow each other in a gentle slope throughout the simulation. Though, at any time during the simulation the accumulated oil volume in Case 2 is higher than in Case 1. After 400 days the accumulated oil volume is 15700 m^3 in Case 1, in Case 2 it has reached 17000 m^3 oil at the same time. This means an increase of 1300 m^3 oil when CO_2 is injected into the reservoir. Water breakthrough occurs after only 2.7 and 2.9 days for Case 1 and Case 2 respectively. After water breakthrough, the accumulated water volume increases rapidly for both cases. As seen from Figure 6-4 Case 2 has higher accumulated water volume than Case 1. After 400 days the difference in the accumulated water volume is 37500 m^3, as 318000 m^3 water is produced in Case 1 and 355500 m^3 is produced in Case 2. This large volume flow of water is due to no restrictions for the fluids to flow through the fractured zone in the reservoir, consequently most of the oil and water are produced from the second zone. This is seen in Figure 6-5, where the total liquid flowrate in the different sections in the pipe is displayed. The plot represents Case 2 after 400 days.

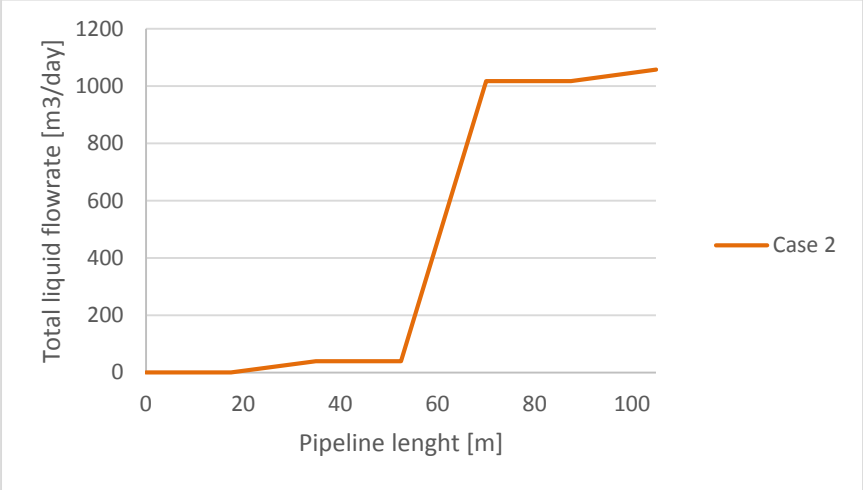

Figure 6-5: Total liquid volumetric flowrate in the pipe, Case 2.

The total liquid flow includes the volume of oil, water and CO_2. Case 2 simulates injection of CO_2 into the reservoir, hence CO_2 is produced along with the water. The plot in Figure 6-5 shows that the major part of the total liquid volume is produced in the fractured part of the reservoir, as it enters the pipe in section 4. Thus CO_2-injection into a fractured carbonate reservoir is unprofitable, due to the injected CO_2 will flow through the fractures and directly into the production well. Also, due to the very early breakthrough of water, significant amounts of the injected CO_2 will be recycled with the produced water. This is clearly indicated in Figure 6-6, which displays the graphical output of the water cut in the pipe for Case 2 during the whole simulation.

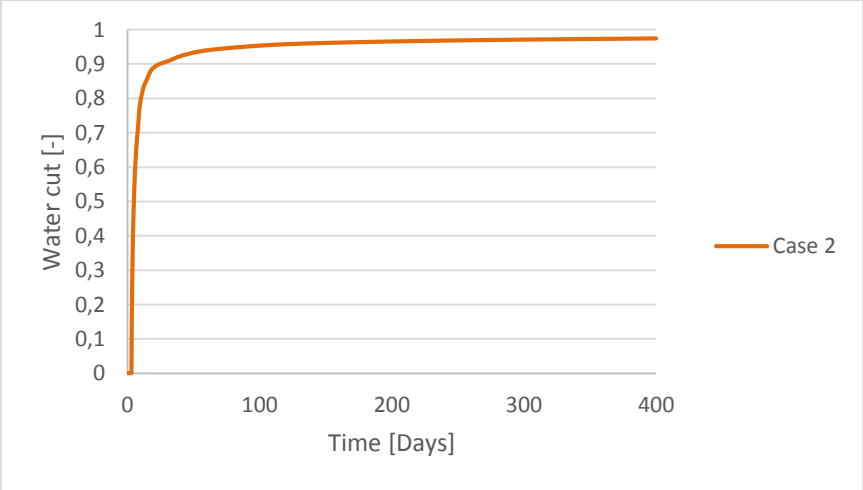

Figure 6-6: Graphical output of the water cut, Case 2.

The water cut is the water/oil ratio and expresses the amount of water produced along with the oil. The water cut in Case 2 is 0.975 after 400 days of simulation, meaning that 97.5 % of the total liquid volume is water and CO_2. The high value for the water cut results in low quality oil and large amounts of water to be removed subsequently.

6.3 Oil production from a heterogeneous carbonate reservoir with closed valve in the fractured zone

This subchapter focuses on the oil and water production from a carbonate reservoir with fracture. The aim is to study how closing of the fractured zone affects the oil and water production from the reservoir. Two different cases were simulated, Case 3 and Case 4. For both cases the control valve in the second production zone is closed, so that the production of oil and water from the fractured zone is completely stopped. The oil and water production from the well will continue from the other production zones in the reservoir. Case 3 simulates water displacing the oil by waterflooding. Case 4 simulates injection of CO_2 into the reservoir, and simulates CO_2 displacing the oil. Figure 6-7 shows the accumulated oil and water production in the two cases. The blue lines represent Case 3, the black lines represent Case 4, the solid curves represent oil and the dotted curves represent water.

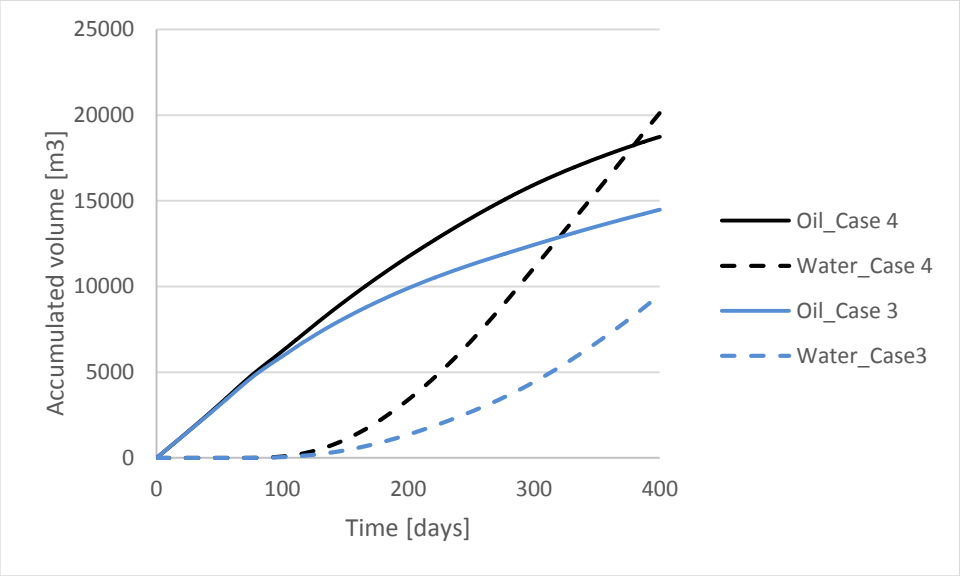

Figure 6-7: Accumulated oil and water, Case 3 and Case 4.

At the beginning, when water and CO_2 are flooded into the reservoir, the accumulated oil volume increases steadily for both cases. Oil flows more easily with CO_2-flooding compared to waterflooding, and after 46 days the accumulated oil volume in Case 4 starts to follow a steeper slope than the accumulated oil volume in Case 3. Water breakthrough occurs approximately at the same time for the two cases, respectively after 65 days for Case 3 and after 64 days for Case 4. When the water production starts, the accumulated water volume in Case 2 increases more rapidly than in Case 1. This results in higher accumulated water volume for Case 2 than for Case 1 throughout the simulation. The accumulated oil volume is increased by 4200 m^3 when CO_2 is injected into the reservoir, from 14500 m^3 oil in Case 3 to 18700 m^3 in Case 4. The accumulated water volume increases from 9500 m^3 water

produced in Case 3 after 400 days to 20100 m^3 water produced in Case 4. This means an increase of 10600 m^3 water for the simulation with CO_2-injection. Due to the closed control valve in the fractured zone, the oil and water production mainly occur in the first and the third production zone in the reservoir. Figure 6-8 shows the total liquid flowrate in the pipe for Case 4.

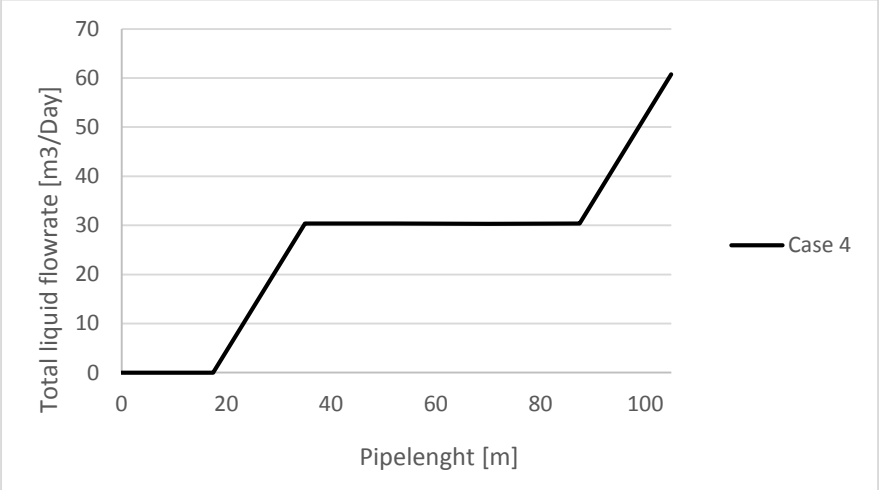

Figure 6-8: Total liquid flowrate in the pipe, Case 4.

As seen from Figure 6-8 the total liquid flowrate increases along with the pipeline. The inflow from the annulus to the pipe occurs in section 2 and section 6. This is as expected since these sections represent the first and the third production zone in the reservoir. In section 1, 3, 4 and 5 the total liquid flowrate is constant, this due to no inflow from the annulus into the pipe in these sections, as the control valve in the second production zone is closed.

Fractured carbonated reservoirs are a major challenge for the oil industry using CO_2-EOR. The low permeability and the high heterogeneity result in high production rate of water and CO_2, mainly through the fractured zone. By chocking the high permeability zone, the oil and water production will become reduced. On the second hand the water breakthrough will be delayed, resulting in decreased water/oil ratio. Figure 6-9 shows the water cut in Case 3 and Case 4 during the whole simulation.

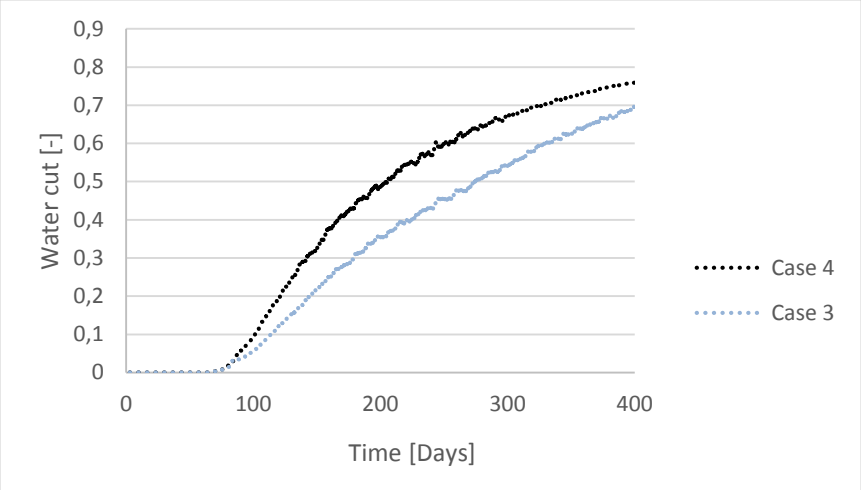

Figure 6-9: Graphical output of water cut, Case 3 and Case 4.

Immediately after water breakthrough, the water cut in Case 4 has a steeper increase than the water cut in Case 3. But, after short time the water cut curve for Case 4 is slowed and flattens out, while Case 3 continues to rise throughout the simulation. At the end of the simulation, after 400 days, the water cut in Case 4 is 0.725 and the water cut in Case 3 is 0.654

6.4 CO_2 distribution in a carbonate reservoir rock

In this subchapter the results from the cases with CO_2-injection are reviewed and compared to investigate how CO_2 is distributed in the carbonate reservoir. The plots are generated using the software-tool Techplot RS. Techplot RS visualizes the results from the reservoir simulations and models the fluid flow through the specified reservoir.

6.4.1 Distribution of CO_2 and water after water breakthrough

Figure 6-10 shows the oil saturation scale used in the results generated from Techplot RS. The color goes from red to dark blue, where red color indicates oil saturation of 1.0 and dark blue color indicates an oil saturation 0.2.

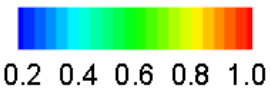

Figure 6-10: Oil fraction scale used in the results generated by Techplot RS.

Figure 6-11 shows the oil saturation in the reservoir, initially and after water breakthrough for all three cases. For the simulations it is assumed that CO_2 is injected into the water phase, and therefore this water phase is represented as carbonated water.

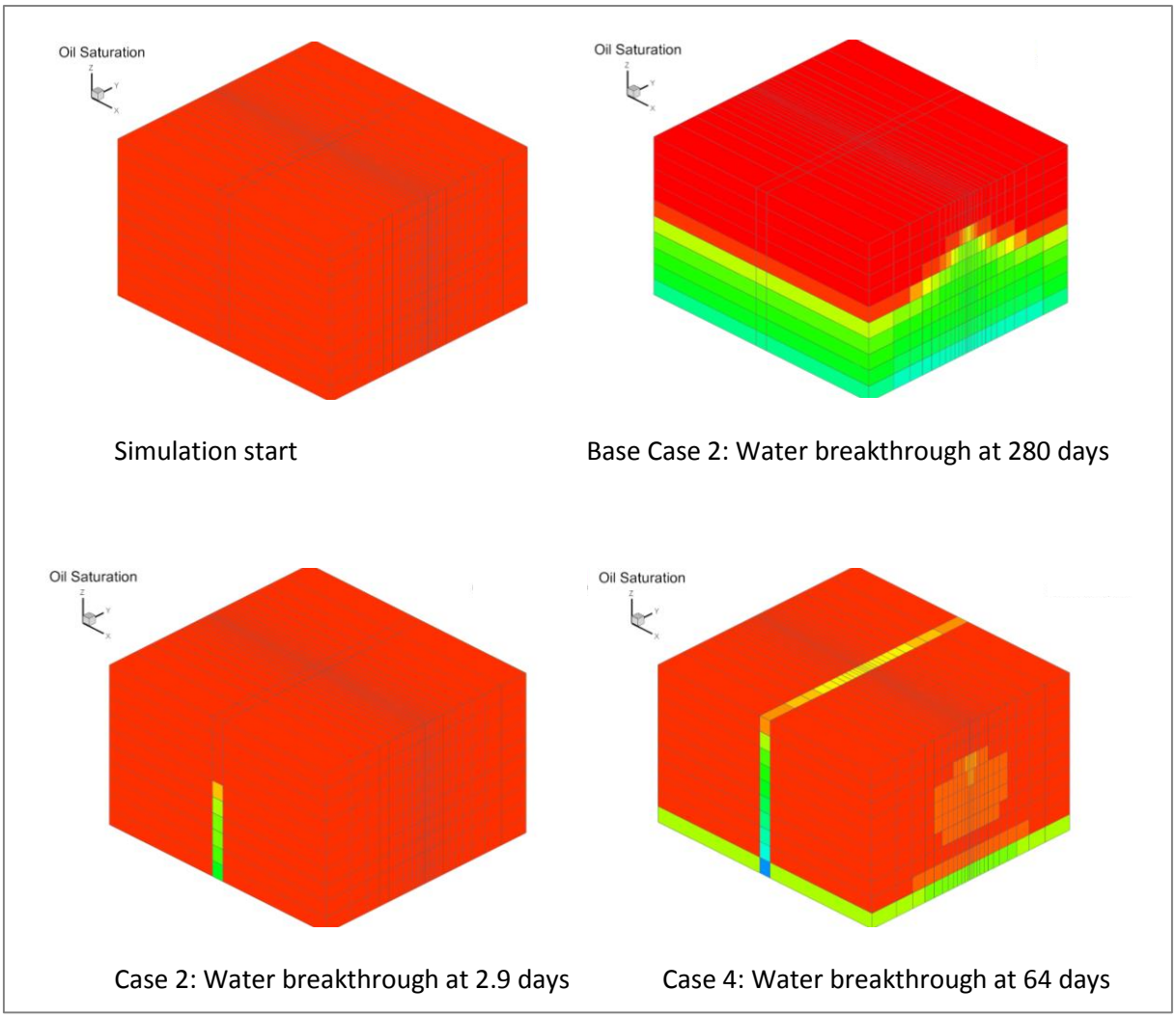

Figure 6-11: Saturation of oil initially and at water breakthrough.

Carbonated water goes upward, from the bottom of the reservoir towards the production well. Water breakthrough happens at different time for the three cases. In Base Case 2 the water breakthrough takes place in the entire reservoir at the same time, after 280 days. In Case 2 and Case 4 the water breakthrough takes place in the second production zone, this is because of the high permeability specified for this zone. After only 2.9 days the water breakthrough occurs in Case 2. As seen from Figure 6-11 the carbonated water flows straight through the fracture and into the production well, without distribute in the reservoir. In Case 4 the water breakthrough occurs after 64 days. Due to the chocking of the fractured zone in Case 4, the carbonated water distributes within the reservoir. This is more easily seen in the 2D-plot displayed in Figure 6-12.

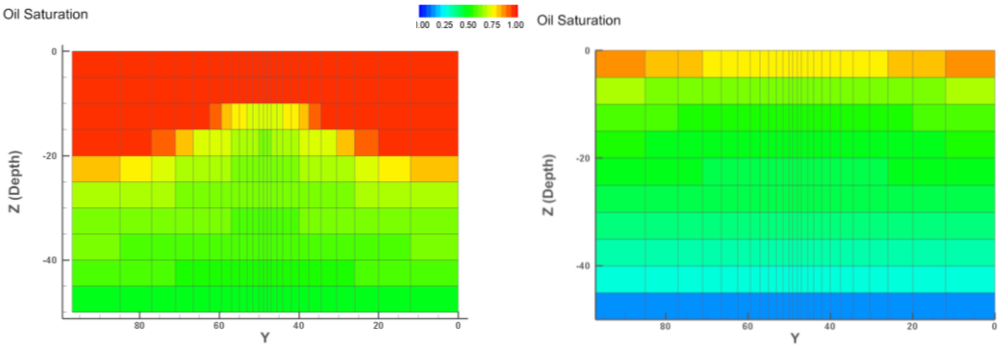

Case 2: Water breakthrough at 2.9 days Case 4: Water breakthrough at 64 days

Figure 6-12:2D view at water breakthrough in the second production zone.

From the 2D-plots of the oil saturation in the second production zone, it is seen that the carbonated water in Case 2 flows straight through this zone without disperse into the other zones. The well is located in the third grid block in z-direction, and the oil saturation decreases from this position and downwards in the production zone. Subsequently, the oil saturation is high in the area above and around the production well. This is due to the pressure difference between the reservoir and the wellbore. In Case 4 the oil saturation in the second production zone is more evenly distributed due to the closed valve.

6.4.2 Distribution of CO_2 and water after 400 days

Figure 6-13 shows the distribution of CO_2 and water in the reservoir for Case 2 and Case 4 after 400 days of production.

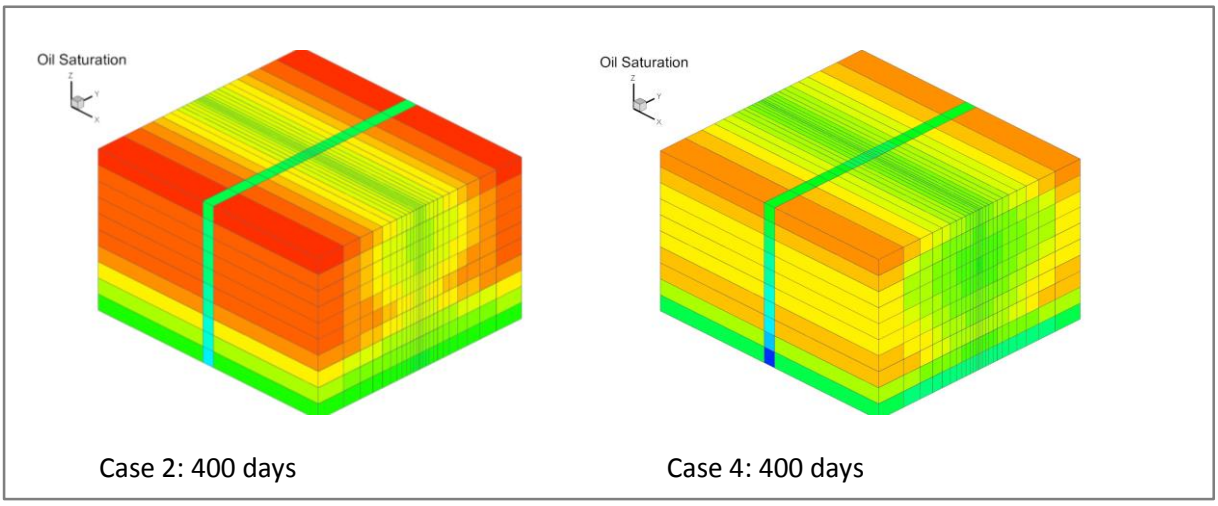

Case 2: 400 days Case 4: 400 days

Figure 6-13: Saturation of oil after 400 days.

From Figure 6-13 it is seen that Case 4 shows good distribution of carbonated water in the reservoir compared to Case 2. This is due to closing of the fractured zone in Case 4, causing the carbonated water to disperse from the high permeable zone to the low permeable

neighbor zones. For Case 2 the carbonated water flows directly into the production well, causing low production from the other zones in the reservoir and large amounts of the injected CO_2 to be recycled. This is also seen in the 2D-plots of the second production zone in Figure 6-14. The plots represent the saturation of oil after 400 days of production.

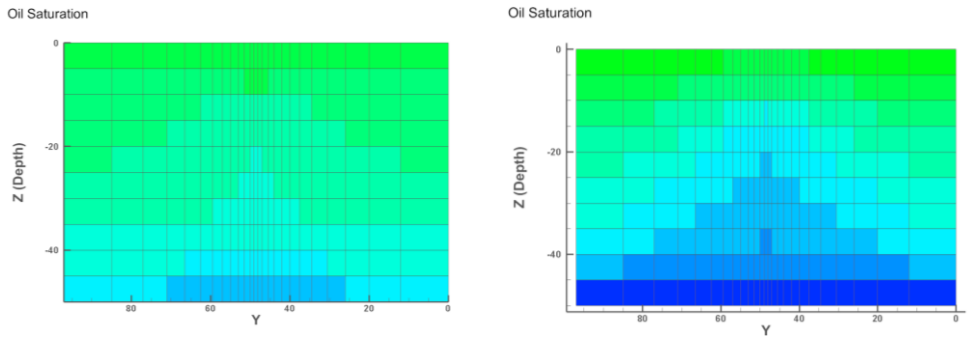

Case 2: 400 days Case 4: 400 days

Figure 6-14: 2D view in the second production zone after 400 days of production.

The closed valve in Case 4 allows the CO_2 to be in contact with the oil within the reservoir. CO_2 acts as a solvent that reduces the oil viscosity and enables the oil to flow into the production well. As seen, closing the fractured zone of the reservoir results in good distribution..

7 Discussion

In this chapter the results from the simulations are summarized and discussed.

CO_2- EOR is an attractive method because of its potential to increase the oil production from matured oilfields, and at the same time reduce the carbon footprint from the industrial sources. The petrophysical properties of the reservoir determine the effectiveness of the CO_2-injection. Reservoir properties affect the field response to CO_2-EOR, including the oil production rate, and the CO_2 recycle ratio and the CO_2 distribution in the reservoir. The base case simulations indicate that oil recovery is improved when CO_2 is injected into the reservoir. Simultaneously the water production is increased. Although the CO_2-injection increases the amount of oil and water produced from the reservoir, the total production volume is small. This is due to the low permeability specified for the production zones in the reservoir. In Table 7-1 the results from the performed simulations are summarized.

Table 7-1: Summarize of results from the different cases.

	Accumulated oil volume [m^3]	Accumulated water volume [m^3]	Water Breakthrough [day]	Water cut
Base Case 1	20 000	7 500	N/A	N/A
Base Case 2	25 000	11 500	280	N/A
Case 1	15 700	318 000	2,7	N/A
Case 2	17 000	355 500	2,9	0.975
Case 3	14 500	9 500	65	0.654
Case 4	18 700	20 100	64	0.725

Carbonate reservoirs are characterized by high variety in their petrophysical properties within small sections of the reservoir. Most carbonate reservoirs are naturally fractured. The high heterogeneity is one of the main reasons for the low oil recovery from these reservoirs. Water flows more easily through the fractured zone compared to the oil, resulting in very early water breakthrough and thereby high water and low oil flowrate. Closing the fractured zone in the reservoir will solve the problem with high water production, see Figure 7-1 and Figure 7-2.

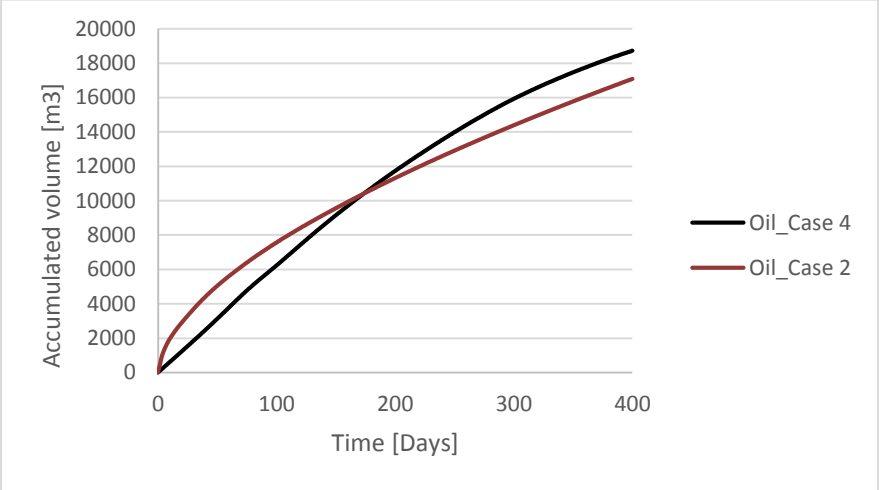

Figure 7-1: Accumulated oil volume, Case 2 and Case 4.

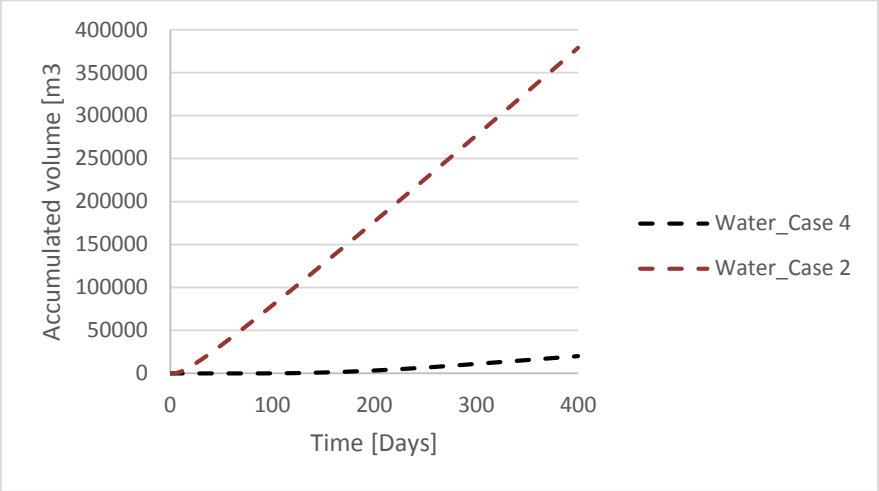

Figure 7-2: Accumulated water volume, Case 2 and Case 4.

Water produced along with the oil results in difficulties for the oil industry, both in an economic, operational and environmental way. Treatment of the produced water faces challenges resulting in necessity for expanding the capacity of water separation and facilities for handling the large volumes of water. The results indicate that carbonate reservoirs with fractures have low oil production, high water production and early breakthrough of water. As seen, closing the fractured zone will give significantly reduced water production and increased oil production over time.

Fractures in the reservoir are a major problem for the oil industry, especially using CO_2-EOR. The consequence with injection of CO_2 into fractured reservoirs, is that the carbonated water or supercritical CO_2 moves through the fractures and directly into the production well, without getting distributed in the reservoir. Large amounts of CO_2 will be reproduced and will not contribute to EOR. Figure 7-3 shows that a major part of the total liquid flow goes through the fractured zone in the reservoir.

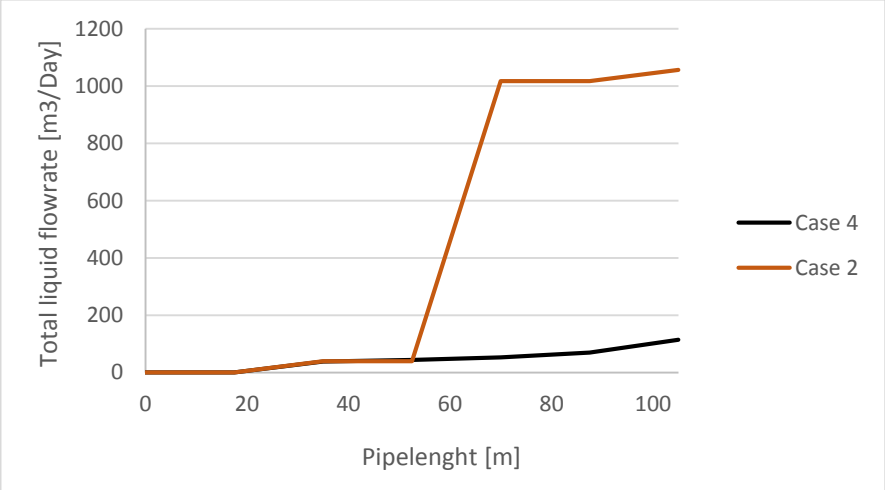

Figure 7-3: Total liquid flowrate along the pipe, Case 2 and Case 4.

Produced water is the largest by-product associated with the oil production. Injection of CO_2 into a fractured reservoir is to no purpose, due to high CO_2 recycle ratio. Assuming the injected CO_2 is dissolved in the water phase, water is considered as carbonated water. Thus the water cut shown in Figure 7-4 represents the ratio of carbonated water to the total liquid.

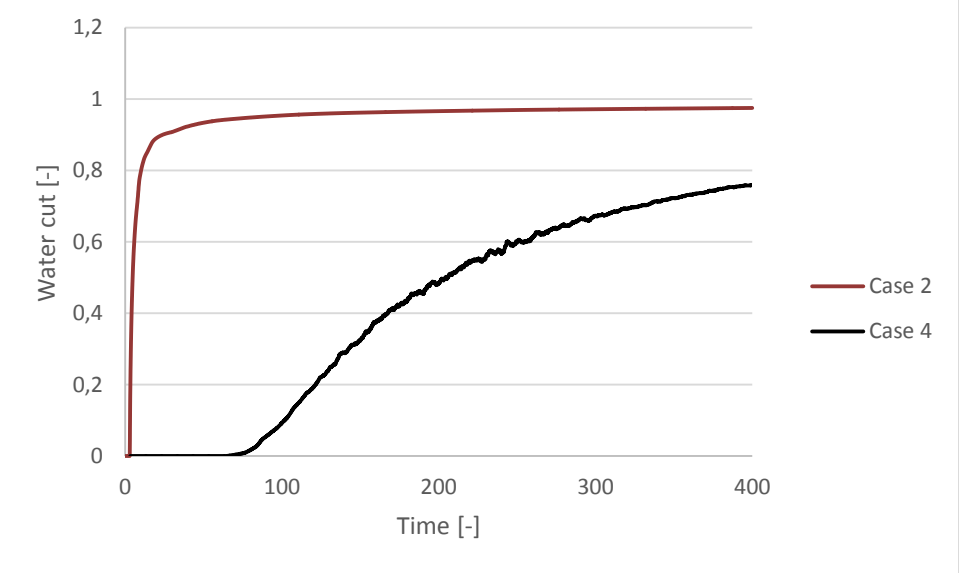

Figure 7-4: Water cut, Case 2 and Case 4.

Closing the fractured zone is crucial to introduce CO_2- EOR to a heterogeneous carbonate reservoir. The oil industry aim for new inflow control technology to shut off production from highly fractured zones, and thereby be able to utilize the benefits from CO_2-injection. Figure 7-4 shows that closing the fractured zone reduces the water cut dramatically. This is advantageous to achieve improved oil quality as well as lower production and separation costs.

8 Conclusion

The objective of this Master's thesis was to study injection of CO_2 into a carbonate reservoir. The study included near-well simulations of oil production and CO_2-distribution, using the reservoir software Rocx in combination with OLGA. The reservoir were characterized by low permeability and high heterogeneity. Four different cases were simulated for an oil-wet rock with fractures. The fractured part of the reservoir was simulated as a high permeability zone, thus the permeability was set much higher in this zone compared to the other zones in the reservoir. To investigate the distribution of CO_2 in the reservoir, it was necessary to choke the production from the fractured zone in two of the performed cases. This was done by closing the control valve in the specified production zone. In addition to the simulations of a fractured reservoir, two cases were simulated for a reservoir without fractures. These simulations were performed to study how the CO_2-injection affects the amount of oil produced.

CO_2-injection into a carbonate reservoir increases the oil recovery, but simultaneously the water production is increased.

The petrophysical properties of the reservoir significantly affect the field response of CO_2-EOR. Carbonate reservoirs with fractures have low oil production, high water production, early water breakthrough and high water cut.

CO_2-injection into fractured reservoir causes small changes in the oil production but it greatly affects the water production. The enormous amounts of water produced results challenges regarding the necessity for expanding the capacity of water separation and facilities for handling the large volumes of water.

Water breakthrough occurs after only 2.9 days in a fractured reservoir and the water cut is 97.5 %. Closing the fractured zone causes delayed water breakthrough and dramatically reduced water cut, resulting in improved oil quality as well as lower production and separation costs.

The simulations indicate that CO_2-injection into a carbonated reservoir in combination with closing of fractured zones result in good distribution in the reservoir.

9 References

[1] Ettehadtavakkol, Amin and Lake, Larry W. and Bryant, Steven L. (June 2014). CO_2-EOR and storage design optimization. *International Journal of Greenhouse Gas Control*, Vol. 25, page 79-92.

[2] Hill, Bruce and Hovorka, Susan and Melzer, Steve (2013). Geologic carbon storage through enhanced oil recovery. *Energy Procedia*, Vol. 37, p. 6808-6830, USA: Elsevier Ltd.

[3] Khudaida, Kamal Jawher and Das, Diganta Bhusan (December 2012). A numerical study of capillary pressure-saturation relationship for supercritical carbon dioxide (CO_2) injection in deep saline aquifer. *Chemical Engineering research and Design*, Vol. 92, Issue 12, page 3017-3030.

[4] Tarek, Taifu Ahmed (2014). Petrophysical characterization of the effect of Xanthan gum on drainage relative permeability characteristics using synthetic unconsolidated core plugs. *Degree of Master of Petroleum Engineering*, Dalhousie University, Halifax: Faculty of Engineering.

[5] Brettvik, Majken (2013). Eperimental and computational study of CO_2 for EOR and secure storage reervoirs. *Master Thesis*, Telemark University College, Faculty of Technology.

[6] Fitch, Peter James Rowland. (2010). Heterogeneity in the petrophysical properties of carbonate reservoirs. *Doctor of philosophy*, The University of Leicester, Department of Geology.

[7] China Oilfield Technology (2013). Three Phases of Oil Recovery. *Annual Report 2013*, Available from: http://www.chinaoilfieldtech.com/oilrecovery.html.

[8] Kulkarni, Madhav M. (2003). Immiscible and miscible gas-oil displacements in porous media. *Master of Science in Petroleum Engineering*, The Graduate Faculty of the Louisiana State University and Agricultural and Mechanical College: The Craft and Hawkins Department of Petroleum Engineering.

[9] Ahmed, Kamal (2013). CO_2 injeksjon for økt oljeutvinning i kalk. *Masteroppgave i reservoarfysikk*, Universitet i Bergen: Institutt for fysikk og teknologi.

[10] Oil and Gas 360 (02.02.2016). *Enhanced Oil Recovery Can Reduce World's Carbon Emissions: Western Governors.* Available from: http://www.oilandgas360.com/enhanced-oil-recovery-can-reduce-worlds-carbon-emissions-western-governors.

[11] Pasala, Sangeeta M. (2010). CO2 displacement mechanisms: Phase equilibria effects and Carbon dioxide sequestration studies. *Doctor of Philosophy,* The University of Utah: Department of Chemical Engineering.

[12] NRG Energy (2014). CO_2 Enhanced Oil Recovery. *NRG Fact Sheet,* Texas: NRG Energy Inc., Available from: http://www.nrg.com/documents/business/pla-2014-eor.pdf

[13] Ghoodjani, E. and Bolouri S.H. (2011). *Experimental study and calculation of CO_2-oil relative permeability*, 53-(2) page 123-131, Iran: Petroleum & Coal Sharif University of Technology and Shahid Bahonar University. ISSN 1337-7027.

[14] Tiab, Djebbar and Donaldson, Erle C. (2012). *Petrophysics, Theory and Practice of Measuring Reservoir Rock and Fluid Transport Properties*, Third edition, USA : Gulf Professional Publishing. ISBN: 978-0-12-383848-3.

[15] Oljeindustriens Landsforening (2013). Innføring i Geologi. *Faktahefte for Utdanning til olje og gassindustrien*, Utforming: Finnestad AS. Available from: http://www.utog.no/postmann/dbase/bilder/geologihefte-web.pdf

[16] Marshak, Stephen (2007). *Earth Portrait of a planet*, Third edition, W.W. Norton & Company Inc. ISBN 978-0-393-93036-8.

[17] Hyne, Norman J. (2001). *Nontechnical Guide to Petroleum Geology, Exploration, Drilling and Production*, Second edition, USA: Penn Well Corporation. ISBN: 0-87814-823-X.

[18] Selley, Richard C. (1998). *Elements of Petroleum Geology,* Second edition, USA: Academic Press California. ISBN: 0-12-636370-6.

[19] San Joaquin Valley Geology (02.02.2016). *Oil Geology of the San Joaquin Valley.* Available from: http://www.sjvgeology.org/geology/oil_geology.html

[20] Dandekar, Abhijit Y. (2013). *Petroleum Reservoir Rock and Fluid Properties*, Second edition, USA: Taylor & Francis Group LLC. ISBN: 978-1-4398-7636-7.

[21] Kvinge, Glenn-Andre Dåtland (2012). En eksperimentell studie av CO_2 lagring i sandstein og kalkstein med bruk av ulike avbildningsteknikker. *Masteroppgave i reservoarfysikk*, Universitet i Bergen: Institutt for Fysikk og teknologi.

[22] Encyclopædia Britannica (02.02.2016). *Porosity.* Available from: http://global.britannica.com/science/rock-geology#ref618624

[23] Gibson, Maria. Porosity and Permeability. *Groundwater Geek.* Available from: http://www.groundwatergeek.com/groundwater/porosity

[24] The Geological Society (02.2.2016). *Compaction and Cementation.* Available from: http://www.geolsoc.org.uk/ks3/gsl/education/resources/rockcycle/page3559.html

[25] International Human Resources Development Corporation. (02.02.2016). IPIMS, e-learning for the Upstream Petroleum Industry, Irreducible water. Available from: www.ihrdc.com/els/ipims-demo/t26/offline_IPIMS_s23560/resources/data/G4108.htm

[26] Satter, Abdus and Iqbal, Ghulam M and Buchwalter, James L. (2007). *Practical Enhanced Reservoir Engineering, Assisted with Simulation Software*. USA: PennWell Corporation. ISBN-13: 987-1-59370-056-0. ISBN-10: 1-59370-056-3.

[27] HIS Energy, Available from: http://www.fekete.com/SAN/WebHelp/FeketeHarmony/Harmony_WebHelp/Content/HTML_Files/Reference_Material/General_Concepts/Relative_Permeability.htm

[28] Schlumberger (Summer 2007). Fundamentals of Wettability. *Oilfield Review*, number 2, Volume 19, page 66-71.

[29] Mexico Institute of Mining and Technology (02.02.2016). *Capillary Pressure,* Engler571, Chapter 7, Petroleum Engineering Department. Available from: http://infohost.nmt.edu/~petro/faculty/Engler571/Chapter7-Capillarypressure.pdf.

[30] Schille, Arne Kristian (2009). Simulering og Analyse av 3-fase Strømningseksperimenter. *Masteroppgave*, Universitetet i Bergen, Institutt for fysikk og Teknologi.

[31] Mexico Institute of Mining and Technology (02.02.2016). *Permeability,* Engler524, chapter 2a, Petroleum Engineering Department. Available from: http://infohost.nmt.edu/~petro/faculty/Engler524/PET524-2a-permeability.pdf.

[32] Petroleum Inc. (02.02.2016). *Oil and Gas Fundamentals*, Reservoir Rock. Available from: http://www.mpgpetroleum.com/fundamentals.html

[33] Arizona State University (02.02.2016). Introduction to Physical Geography, Hydrology. Available from: https://www.asu.edu/courses/gph111/Hydrology/PorousPermeable.jpg

[34] Glover, Paul W.J. (2013). Formation Evaluation. *MSc. Course notes,* University of Aberdeen, UK, Department of Geology and petroleum Geology.

[35] Moore, Clyde H. (1989). *Carbonate Diagenesis and Porosity*, Vol.46, USA:Elsevier Science Publishers B.V. ISBN: 0-444-87415-1.

[36] Esfahani, Maohammad Reza and Haghigi, Manouchehr. (2004). Wettability evaluation of Iranian carbonate formations. *Journal of Petroleum Science Engineering*, Vol. 92, Issues 2-4, page 257-265.

[37] Tangen, Mathias (2012). Wettability Variations within the North Sea Oil Field Frøy. *Master Thesis,* Norwegian University of Science and Technology, Department of Petroleum Engineering and Applied Geophysics.

Appendices

Appendix A: Task description

Appendix B: Simulation of CO_2 injection in fractured oil reservoir

Paper published in *Linköping Electronic Conference Proceedings 2015 (119) s. 347-355*

Appendix C: Simulation of oil production in a Water-wet reservoir

Appendix D: Calculating Corey exponent in CO_2 injection

Appendix A

Task description

Telemark University College
Faculty of Technology

FMH606 Master's Thesis

Title: Simulation of oil production and CO_2-distribution in carbonate reservoir

TUC supervisor: Britt M. E. Moldestad

External partner: InflowControl AS, Haavard Aakre

Task background:
Production of fossil fuels will be required for many years to meet the high demand of energy worldwide. CO2-EOR has been widely studied the last 40 years and are already in use in several countries. CO2-EOR increases oil recovery by injecting CO2 into the reservoir. CO2 injection will maintain the pressure, mobilize the oil and release petroleum resources that would otherwise be inaccessible. In addition to increased oil recovery, CO2-EOR has the ability to lower the emission of CO2 by storing the gas permanently underground after it is utilized. At well-selected storage sites the rock formation are likely to preserve more than 99 % of the injected CO2 for over 100 years. This is an environmental friendly win-win situation where both oil recovery is increased and the emission of greenhouse gases to the atmosphere is reduced. The physical properties of the oil reservoir rock determine the effectiveness of the CO_2 injection for the EOR-storage process. Reservoir properties affect the field response to the CO_2-storage process, including oil production rate, CO_2 utilization factor and CO_2 recycle ratio.

Task description:
The project will focus on:

1. Literature study:
   - CO_2-EOR
   - CO_2 storage capacity in carbonate reservoirs
   - Petrophysics and rock properties in carbonate reservoirs
2. Simulations of oil production with OLGA/Rocx in fractured carbonate reservoirs:
   - Oil and water wetted rock
   - CO_2-injection
   - Distribution of CO_2

Practical arrangements:
Necessary software will be provided by TUC.

Student: Nora Cecilie Furuvik

TUC Supervisor: Britt Moldestad

Address: Kjølnes ring 56, NO-3918 Porsgrunn, Norway. **Phone:** 35 57 50 00. **Fax:** 35 55 75 47.

Appendix B

Simulation of CO_2 injection in fractured oil reservoir

Paper published in: *Linköping Electronic Conference Proceedings 2015 (119) s. 347-355*

Simulation of CO_2 injection in fractured oil reservoir

Nora I. Furuvik [1] Britt M. Halvorsen [1]

[1]Department of Technology, Telemark University College, Norway,
{Nora.C.I.Furuvik@hit.no,Britt.Halvorsen@hit.no

Abstract

CO_2-EOR is an attractive method because of its potential to increase the oil production from mature oilfields and at the same time reducing the carbon footprint from industrial sources. CO_2-EOR refers to a technique for injection of supercritical-dense CO_2 into oil reservoirs. Remaining oil from mature oil fields has been successfully produced using CO_2-EOR since early 1970's. The reservoir properties together with fluid properties significantly affect the CO_2-EOR performance. This study focuses on CO_2 injection in carbonate reservoirs including simulations of CO_2-distribution in the rock. Carbonate reservoirs are characterized by low permeability and high heterogeneity causing significant amount of CO_2 to be recycled. The simulations are carried out using commercial reservoir simulation software. Criteria for the performed simulations are a highly heterogeneous carbonate reservoir with fractures. The simulations show that CO_2-injection in combination with closing of fractured zones result in high oil production and good distribution of CO_2 in the reservoir.

Keywords: CO_2 EOR, fractured reservoir, inflow control, near well simulations

1 Introduction

Production of fossil fuels (oil and gas) will be required for many years to meet the high demand of energy worldwide. CO_2-EOR or CO_2-flooding has been widely studied the last 40 years and are already in use in several countries. CO_2-EOR increases oil recovery by injecting CO_2 into the reservoir, either in form of supercritical CO_2 or as carbonated water. CO_2 injection will maintain the pressure, mobilize the oil and release petroleum resources that would otherwise be inaccessible (Jakobsen et al, 2005).

In addition to increased oil recovery, CO_2-EOR has the ability to lower the emission of CO_2 by storing the gas permanently underground after it is utilized. At well-selected storage sites the rock formation are likely to preserve more than 99 % of the injected CO_2 for over 100 years (NETL/DOE, 2010). This is an environmental friendly win-win situation where both oil recovery is increased and the emission of greenhouse gases to the atmosphere is reduced.

The physical properties of the oil reservoir rock (porosity, permeability) determine the effectiveness of the CO_2 injection for the EOR-storage process. Reservoir properties affect the field response to the CO_2-storage process, including oil production rate, CO_2 utilization factor and CO_2 recycle ratio. (Ettehadtavakkol, 2014). This study focuses on CO_2 injection in carbonate reservoirs including simulations of CO_2 distribution in the porous rock. Carbonate reservoirs are characterized by low permeability and high heterogeneity causing significant amount of CO_2 to be recycled. The simulations are carried out using commercial reservoir simulation software. Criteria for the performed simulations are a carbonate reservoir with fractures. The oil production performance from a carbonate reservoir is nearly half the production from sandstone, whereas the CO_2 utilization is about 60% less.

2 Oil recovery

Oil recovery refers to the extraction process of liquid hydrocarbons from beneath the Earth's surface. The extraction process occurs in three different phases; primary, secondary and tertiary oil recovery phase. These three different ways of oil production is illustrated in Figure 1 (China Oilfield Technology, 2013). In the primary phase of oil production, the drive mechanism for oil extraction is the pressure difference between the oil reservoir and the production well. The oil reservoir covers an extended area, thus the reservoir pressure slowly will decline over time. The main pressure drop is located near the production well. Injection of pressurized gas and/or water into the reservoir will rebuild the reservoir pressure and sweep more oil towards the production wells. This recovery phase is known as secondary oil recovery phase or water flooding. After primary and secondary oil recovery phases, there are still significant amounts of oil remained trapped in the reservoir. (Kulkarni, 2003) The remaining oil reserves are trapped in the reservoir pores, and can no longer be forced to migrate toward the production well by water flooding. As oil saturation in the reservoir declines, more oil reserves are trapped by capillary forces or in dead-end pores, resulting in decreased mobility of the remaining oil. (Hill *et al* 2013; Ahmed, 2013; Kulkarni, 2003) At this point, a tertiary phase of oil production can be considered.

Tertiary enhanced oil recovery (EOR) involves techniques for injection of steam (thermal recovery), chemicals (chemical flooding) or miscible gasses (miscible displacement) to improve the properties of the remaining oil in order to make it flow more freely within the reservoir. (Hill *et al* 2013; Ahmed, 2013)

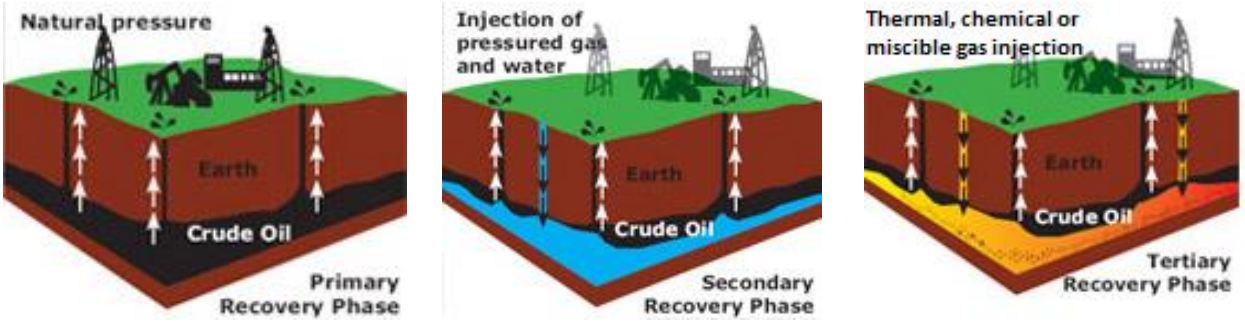

Figure 1. Primary, secondary and tertiary oil production. (China Oilfield Technology, 2013)

The oil viscosity is reduced dramatically with dissolving CO_2 in oil so that the oil flows more freely within the reservoir. When CO_2 comes into contact with crude oil a process of dissolution occurs thereby causing swelling of the oil. This results in expansion in oil volume which means that some fluid has to migrate. The degree of swelling depends on pressure, temperature, hydrocarbon composition and physical properties of the oil. (Pasala, 2010; Melzer 2012; Hill, 2013; Ghoodjani, 2011)

Use of supercritical CO_2 for EOR increases oil supply by mobilizing residual oil trapped in inaccessible void spaces. CO_2-EOR also contributes to minimize the impact of greenhouse gas emission by keeping CO_2 out of the atmosphere, as much of the CO_2 is exchanged for the displaced oil and water in the pores, and remains trapped in the deep rock formations (NRG Energy Inc., 2014)

3 Petrophysics

Petrophysics is the study of porous geologic material, its physical properties and its interactions with fluids (gases, liquid hydrocarbons and aqueous solutions). (Tiab et al, 2012). Since hydrocarbons are light in density compared to water, the hydrocarbons start to migrate in a porous rock containing water. The hydrocarbons move through fault and fractures in the source rock until they are trapped in a reservoir rock. The reservoir rock is overlain by a seal rock, an impermeable rock layer that does not allow fluids to flow through. The oil and gas accumulates in a trap forming a hydrocarbon reservoir. If there is no such trap along the migration route, the oil and gas will continue their migration out to the surface of the Earth. (Oljeindustriens Landsforening). Accumulation of hydrocarbons in such traps is usually found in coarse-grained, permeable and porous sedimentary rocks. Since the pores most often are water-saturated, the migration of hydrocarbons takes place in an aqueous environment. Oil, gas and water will separate according to the density difference once they are caught in the trap. This is illustrated in Figure 2. (Hyne, 2001; Selley, 1998)

Gas accumulates in the highest portion of the trap, forming a free gas cap. Because the specific gravity of the water is considerable higher than oil, the oil floats on the surface of the water and accumulates in the middle of the trap, forming the oil reservoir. Salt water goes to the bottom. However, due to void spaces and tiny openings in the rocks, capillary forces resist complete gravitational segregation of the fluid phases. Water is therefore found in small amounts in all zones of the reservoir. (Hyne, 2001; Marshak, 2001; Selley, 1998)

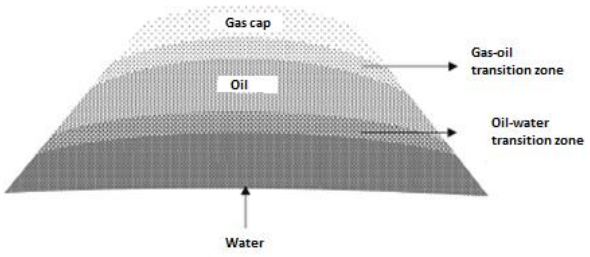

Figure 2. Cross section of a reservoir showing vertical segregation of fluids. (Dandekar, 2013)

3.1 Porosity

A reservoir rock is porous and permeable. For a rock to act as a reservoir it must have pores to store fluids and the pores must be connected to allow transmission of the fluids. Since reservoir rocks are composed of mineral grains and crystals, their properties depend upon the property of the minerals. These properties are highly affected by the reservoir physics, including saturation, relative permeability and porosity. In addition, rock properties also depend on the temperature and pressure, and the type and amount of

contained fluids (oil, gas or water). (Khudaida, et al, 2012).

A porous rock consists of mineral grains and small spaces in between the mineral grains, called void space or pores. Porosity of a rock represents the measure of the void space within the porous rock. Almost all porous material have three basic types of pores; catenary, cul-de-sac and closed pores (Shelley, 1998). A presentation of the three types of pores is given in Figur 3.

Catenary pores include pores connected to other pores with more than one pore channel, Cul-de-sac pores (dead-end pores) are the pores that only connects to other pores through one pore channel. While closed pores include pores that have no connection to other pores at all and are completely isolated from the pore network.

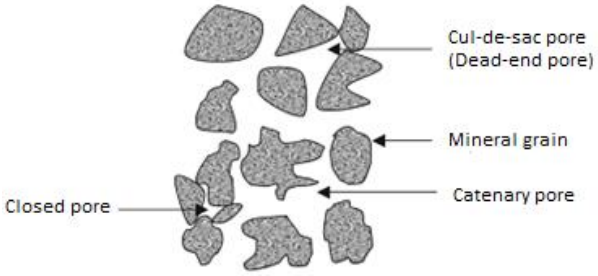

Figure 3. Three basic types of pores. (Dandekar, 2013)

Absolute porosity encompasses all the void spaces, including interconnected pores as well as pores that are sealed off. Absolute porosity is defined as the ratio of the total pore volume (Catenary pores, Dead-end pores and Closed pores) to the bulk volume of the porous rock:

$$\phi_a = \frac{Total\ pore\ volume}{Total\ or\ bulk\ volume} \quad (1)$$

Effective porosity (ϕ) is the proportion of void spaces that excludes the completely disconnected pores (Closed pores). Effective porosity is defined as the ratio of the void volume of interconnected pores (Catenary pores and Dead-end pores) to the bulk volume of the porous rock:

$$\phi = \frac{Void\ volume\ of\ interconnected\ pores}{Total\ or\ bulk\ volume} \quad (2)$$

Thus, effective porosity measures the void volume that is interconnected to the surface. Even if dead-end pores cannot be flushed out, they can still produce oil by pressure depletion or gas expansion. (Khudaida et al, 2012; Tiab et al, 2012; Hyne, 2001; Shelley,1998; Dandekar, 2013)

3.2 Saturation

The void spaces within a reservoir rock are always completely saturated by fluids. However, all available pores are not occupied by hydrocarbon fluids; a certain amount of residual formation water cannot be displaced and is always present in the reservoir. The relative amount of each fluid present in the pores is called saturation. In a hydrocarbon reservoir, oil, gas and water fill a fraction of the total pore volume of the rock (V_{total}):

$$V_{total} = V_{oil} + V_{gas} + V_{water} \quad (3)$$

Fluid saturation is defined as the ratio of the volume occupied by oil, gas or water to total pore volume, which gives following equation for oil saturation (S_{oil}):

$$S_{oil} = \frac{Volume\ of\ oil\ in\ the\ reservoir\ rock}{Total\ pore\ volume\ of\ the\ rock} \quad (4)$$

Similar expressions can be written for gas saturation (S_{gas}) and water saturation (S_{water}).

The endpoint saturations for each fluid phase are of special interest. The most frequently endpoint saturations are irreducible water saturation, residual oil saturation and critical gas- and condensate saturations. The irreducible water saturation defines the maximum water saturation that can retain without producing water. Residual oil saturation is the remaining oil in the reservoir rock at the end of an extraction process or a specific recovery process. (Ahmed, 2012; Tiab et al, 2012; Hyne, 2001; Kvinge, 2012)

3.3 Wettability

Wettability is the tendency for a fluid to spread or adhere to a solid surface in the presence of other immiscible fluids. Wettability has an impact on the capillary forces, relative permeability, irreducible water saturation, residual oil saturation and the interfacial tension. (HIS Energy; Schlumberger, 2007; Ahmed, 2013). Wettability is related to the rock-fluid interactions, thus it is determined by the interaction between the fluids and the rock surface. When two phases are present in a reservoir rock, interfacial tensions exist. For the two immiscible coexisting fluids, the one with lowest interfacial tension is the wetting phase. Interfacial tension relates to the fluid-fluid interactions, and is a measure of the force that holds the surfaces of the two immiscible fluids together. Low rock-fluid interfacial tension means low surface energy and high tendency for the fluid to wet a surface. (Ahmed, 2013).

3.4 Permeability

In addition to being porous, a reservoir rock must have the ability to transmit fluids through its interconnected pores. This rock property is termed permeability, and in Figure 4 it is seen how interconnected pores can give high rock permeability.

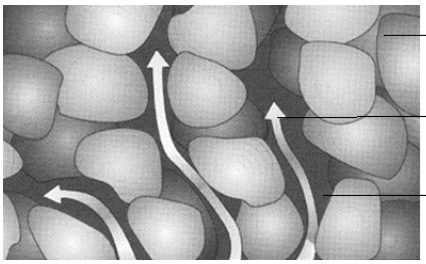

Figure 4. Illustration of a reservoir rocks permeability. (Rocky Mountain Carbon Capture and Sequestration)

Permeability is a measure of how easy a fluid can flow through a porous rock. Permeability is usually expressed in millidarcys (mD). In a 1-dimensional, linear flow, the steady-state flow is calculated according to Darcy's law:

$$Q = A\frac{Kdp}{\mu dx} \quad (5)$$

where K is the permeability of the porous rock [D], Q is the volumetric flow rate [cm^3/s], A is the cross-sectional area of the core sample [cm^2], μ is the viscosity of the fluid [cP], x is the length [cm] and $\frac{dp}{dx}$ is the pressure drop of the core sample [atm/cm].

Absolute permeability defines K when the pores within a reservoir are saturated with one single fluid phase (oil, gas or water). Absolute permeability of a given porous material is a rock property and is independent of the type of fluid.

Effective permeability describes the permeability of each fluid when more than one fluid is present in the reservoir. In a multi-phase system, the permeability highly depends on the relative saturation of each fluid. During the movement through the rock, each fluid will interfere with the other fluids due to capillary forces. These interactions lead to reduction in the flow rate of the each individual phase. Consequently, the effective permeability for each fluid will be lower than the absolute permeability. Multi-phase flow leads to a modification of Darcy's law, by introducing effective permeability instead of absolute permeability:

$$Q_i = A\frac{K_i dp_i}{\mu_i dx} \quad (6)$$

In which i refers to each of the specific fluid phase.

Relative permeability is the ratio of the effective permeability of a particular fluid phase to the absolute permeability, and is given by:

$$K_{rel,i} = \frac{K_i}{K} \quad (7)$$

where $K_{rel,i}$ refers to the relative permeability of the specific fluid phase i. Relative permeability is a dimensionless function. The relative permeability curves in water-wetted and oil-wetted rock are presented in Figure 5 and Figure 6 respectively. S_{orw} represents the residual oil saturation and S_{wc} represents the irreducible water saturation.The plots show that the wettability has significant impact on the shape of the relative permeability curves. The relative permeability curve of the non-wetting fluid has an s-shape, while the relative permeability curve of the wetting fluid is concave upwards.

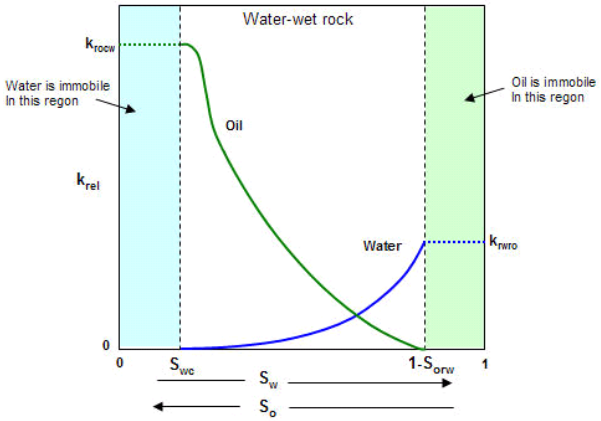

Figure 5. Relative permeability for oil and water in water-wetted rock.

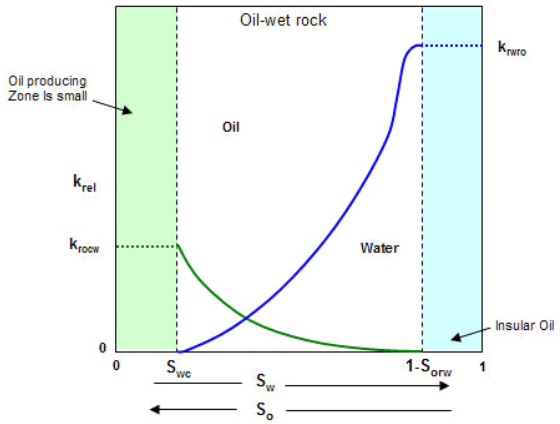

Figure 6. Relative permeability for oil and water in oil-wetted rock.

3.5 CO_2-EOR

Sedimentary rocks are classified by factors like, grain size, sorting, sphericity and porosity. Most oil and gas accumulation have been found in clastic and carbonate reservoirs. The reservoir properties (permeability and heterogeneity in these examples) significantly affect the EOR performance. The low permeability and high heterogeneity of carbonate causes the oil production performance to be small and the CO_2 utilization to be large, compared to sandstone.

CO_2 is usually not miscible on the first contact with the reservoir oil. However, at sufficiently high pressures, CO_2 achieves miscibility with oil for a broad spectrum of reservoirs. Under favorable conditions, the gas will vaporize the low to medium fractions of the reservoir crude. After multiple contacts between the oil and carbon dioxide, a bank of light hydrocarbons and CO_2 will form, and this mixture promotes miscibility

between the CO_2 and the remaining crude oil. Complete miscibility between the oil and CO_2 or hydrocarbon solvents, eliminates interfacial tension and capillary forces and helps to recover, in theory, all of the residual oil. (Pasala, 2010) Supercritical CO_2 is considerably denser than the gaseous CO_2 phase but has lower density and viscosity than the occupant brine saline water in the porous space. As a result of the differences of fluid densities, supercritical CO_2 migrates buoyantly towards the upper confining layer. The preferred depths to inject CO_2 are greater than 800 m (NRG Energy Inc., Texas, 2014) as they provide the required conditions above the critical points of CO_2 for it to stay in supercritical phase. (NRG Energy Inc., Texas, 2014) CO_2 affects the oil and rock by reducing the interfacial tension, reducing the oil viscosity, swelling the oil and by having an acid effect on rock.

4 Simulations

The simulations are carried out using commercial reservoir simulation software, Rocx in combination with OLGA. The OLGA software is the main program, but several additional modules are developed to solve specific cases.

Criteria for the performed simulations are a highly heterogeneous carbonate reservoir with fractures.

4.1 Rocx

Rocx contains detailed information about the geometry of the reservoir. Input parameters to Rocx are reservoir and fluid properties like permeability, porosity, viscosity, initial and boundary conditions. Figure 7 shows the grid and geometry of the simulated reservoir section at initial conditions.

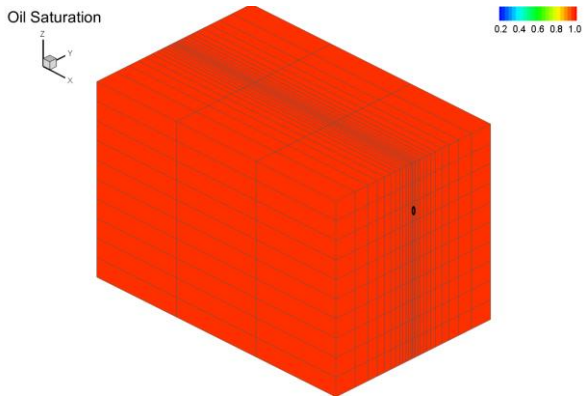

Figure 7. Grid and geometry of the simulated reservoir section.

The geometry of the simulated reservoir is 150 m in length, 106 m in width and 100 m in depth. 3 grid blocks are defined in x-direction, 25 in y-direction and 10 in z-direction. The well is located 70 m from the bottom, as indicated as a black dot in Figure 7. The radius of the wellbore is 0.15 m. The reservoir is divided into three zones in x-direction, where the mid-zone (second zone) represents the fractured part. Thus the permeability is set much higher in this zone compared to the two other zones. The reservoir and fluid properties for this specific case are presented in Table 1.

Table 1. Reservoir and fluid properties.

Properties	*Value*
Oil viscosity	10 cP
Reservoir pressure	176 bar
Temperature	76°C
Gas oil ratio (GOR)	16 Sm^3/Sm^3
Natural gas specific gravity	0.64
Oil specific gravity	0.8
Porosity	0.3
Permeability first zone	100-200 mD
Permeability second zone	10000-20000 mD
Permeability third zone	100-200 mD
Wellbore pressure	136 bar

Data for relative permeability are set manually in table form in Rocx. Oil-wet reservoir is considered in these simulations, and Figure 8 shows the implemented relative permeability curves for oil and water.

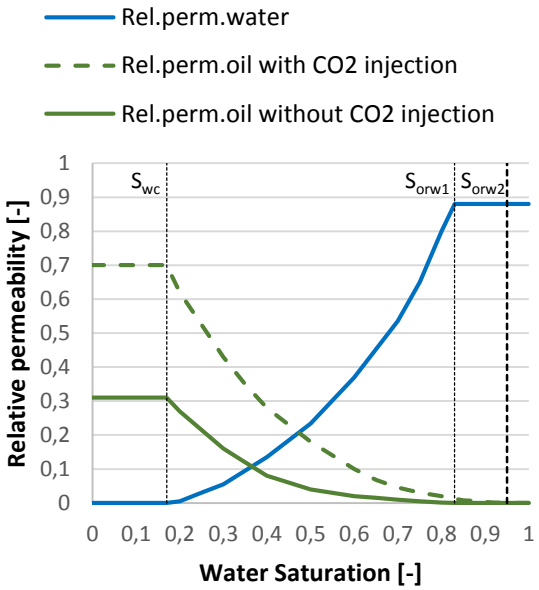

Figure 8. Relative permeability curves in oil-wet carbonate reservoir.

The vertical lines represent the residual oil saturation (S_{orw1} and S_{orw2}) and the irreducible water saturation (S_{wc}). The green lines indicate the relative permeability of oil for two different simulation cases, one where CO_2 is injected to the reservoir (green dotted line) and one without CO_2-injection (green solid line).

The module Rocx is connected to OLGA by the nearwell source, which allows importing the file created by Rocx. In order to get a simulation of a complex fluid flow, OLGA requires both a flowpath and a pipeline. In reality they are the same, but in the simulations the flowpath represents the wellbore and the pipeline represents the annulus. In Figure 9 the sources implemented in the pipeline indicate the inflow from the reservoir into the annulus. The flow from annulus goes through the valves A, B and C and into the wellbore via the leaks. The valves 1, 2 and 3 are simulate packers and are closed during the simulations. Packers are installed to isolate the different production zones in the well.

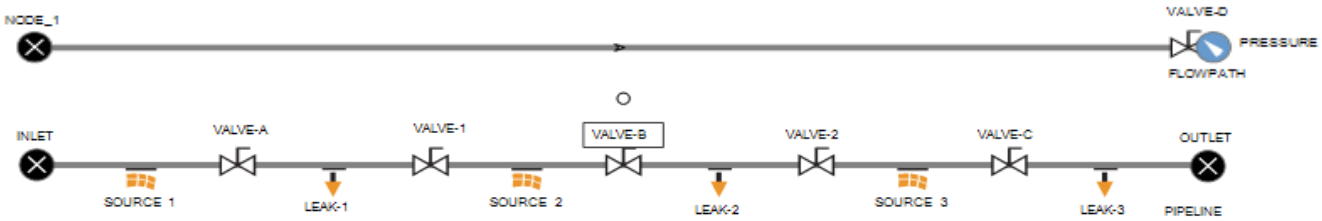

Figure 9. OLGA Study case.

Three different cases (Case 1, 2 and 3) are simulated. The input for simulation in Rocx and OLGA is listed in Table 2. All three cases include the reservoir and fluid properties detailed in Table 1. Case 1 includes the oil relative permeability curve shown as a green solid line in Figure 8. All the valves A, B and C are fully open during the simulation. Case 2 includes the same oil relative permeability curves as for Case 1, but with valve B nearly closed.

In Case 3, CO_2 is injected to the reservoir by assuming that the oil relative permeability curve is significantly changed due to the influence on CO_2 on the fluid properties. The oil relative permeability curve implemented for Case 3 is seen as a green dotted line in Figure 8. Valve B is kept in the same position as for Case 2. The water permeability curve is the same for the three cases and is seen as the blue line in Figure 8. All simulations where run for 300 to 400 days.

Table 2. Input for simulation case 1, 2 and 3.

Simulation Case	*Data input to Rocx*	*Relative permeability curve*	*CO_2injection to reservoir*	*Position Valve A and C*	*Position Valve B*	*Simulation time*
Case 1	See table 1	See Figure 8	No	Open	Open	400 days
Case 2	See table 1	See Figure 8	No	Open	Nearly closed	312 days
Case 3	See table 1	See Figure 8	Yes	Open	Nearly closed	366 days

Fractures in the reservoir are a major problem in oil fields using CO_2-EOR. The consequence is that the injected CO_2 moves through the fractures and directly to the production well without getting distributed in the reservoir. The CO_2 is reproduced and will not have any affection on the oil recovery. The fracture in the reservoir is specified as the high permeability zone (second production zone).

The oil industry focuses on developing improved technology for automatically closing down production from water and gas producing zones.

In this study, Case 2 and Case 3 are simulated with the valve placed in the second production zone (Valve B) nearly closed. OLGA does not allow the valve to be completely closed and therefore a negligible opening is used. In the simulation with Case 1 valve B is fully open.

5 Results

For each case the accumulated volume of oil and water are studied and compared. Figure 10 and Figure 11 show the accumulated volume production as a function of time for oil and water respectively. In Case 1 there are no restrictions for the fluid flow. This results in high production flow of oil and water, mainly through the fractures. Due to the high production rate, the water breakthrough occurs after only 22 days. In Case 2 the high permeability zone is choked, giving low oil production and late water breakthrough (after 260 days). The oil permeability curve in Case 3 is changed to account for the effect of CO_2 injection to the reservoir. Valve B is kept nearly closed, as in Case 2. The accumulated volume of oil increases significantly compared to Case 2, whereas the water breakthrough occurs apparently at the same time.

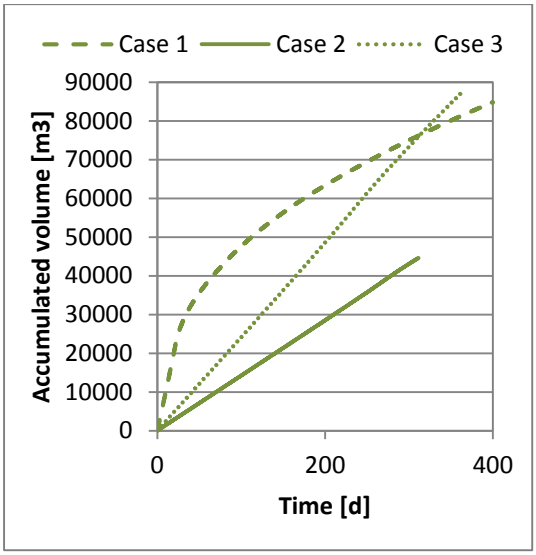

Figure 10. Accumulated volume of oil.

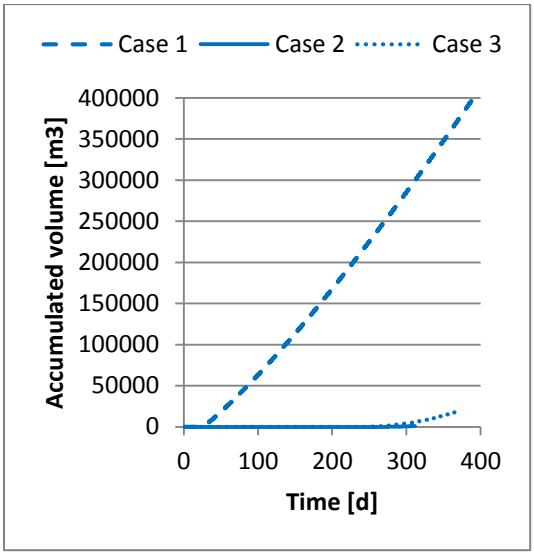

Figure 11. Accumulated volume of water.

In Table 3 the time for water breakthrough in the three different production zones are presented together with the water cut after 310 days of production.

The water cut is defined as the water volume flow divided by the total liquid flow.

Table 3. Water breakthrough and water cut.

Simulation Case	*Water breakthrough in production zone 2[d]*	*Water breakthrough in production zone 1 and 3[d]*	*Water cut after 310 days [-]*
Case 1	22	98	0,8325
Case 2	260	280	0,2378
Case 3	235	240	0,3962

From Table 3 it is seen that after 310 days the water cut are 0.8235 for Case 1, 0.2378 for Case 2 and 0.3962 for case 3. A graphical output of the water cut during the whole simulation is shown in figure 12.

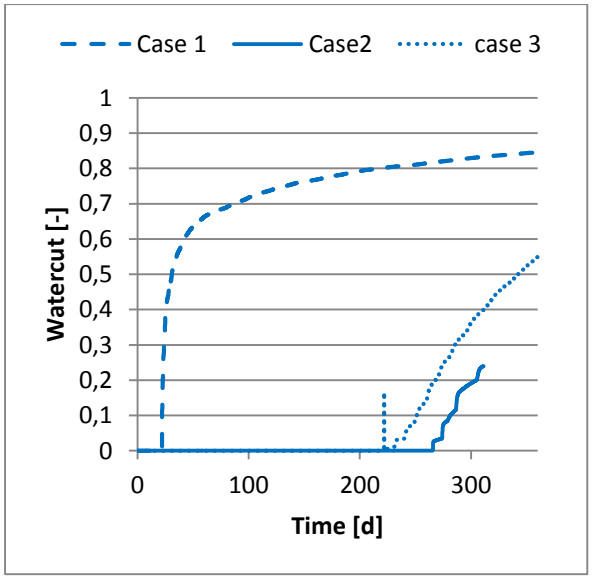

Figure 12. Graphical output of the water cut.

The plots in Figure 12 displays that Case 1 has a high water cut compared to the other cases. This is not economically favorable due to high separation costs and need of very large separation units.

Figure 13 and Figure 14 shows the distribution of water and carbonated water in the reservoir for Case 2 and Case 3 respectively. In Case 3 it is assumed that CO_2 is injected in the water phase, and therefore this water phase is represented as carbonated water. The plots represent the saturation of oil after 312 days of production. As expected, the distribution of water/carbonated water disperses from the high permeable zones to the low permeable neighbor zones in both cases. Case 3 shows high distribution of water in the reservoir compared to Case 2. This is due to injection of CO_2. CO_2 mixes with the oil, making it less viscous and more mobile. The simulations indicate clearly that CO_2 injection in combination with closing of fractured zones result in high oil production and good distribution of CO_2 in the reservoir.

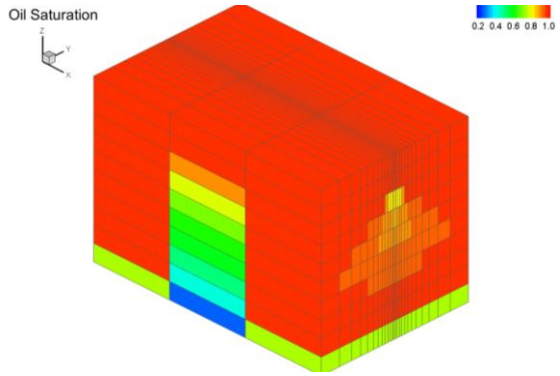

Figure 13. Saturation of oil Case 2 at 312 days.

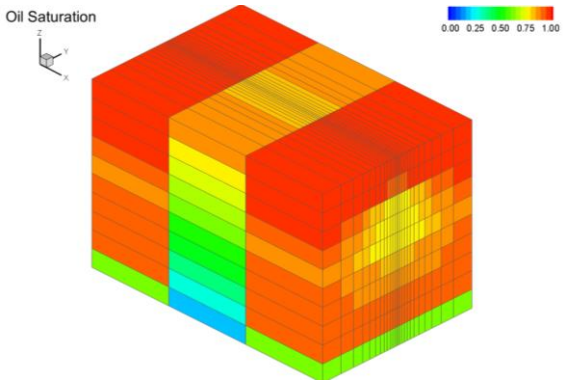

Figure 13. Saturation of oil Case 3 at 312 days.

6 Conclusion

CO_2-EOR is an attractive method because of its potential to increase the oil production from mature oilfields and at the same time reducing the carbon footprint from industrial sources. CO_2-EOR refers to a technique for injection of supercritical-dense CO_2 into an oil reservoir. Remaining oil from mature oil fields has been successfully produced using CO_2-EOR since early 1970's. The reservoir properties (porosity, permeability) together with fluid properties significantly affect the CO_2-EOR performance. This study focuses on CO_2 injection in carbonate reservoirs including simulations of CO_2-distribution in the rock. Carbonate reservoirs are characterized by low permeability and high heterogeneity causing significant amount of CO_2 to be recycled. The simulations are carried out using commercial reservoir simulation software. Criteria for the performed simulations are a highly heterogeneous carbonate reservoir with fractures. The simulations indicate clearly that CO_2 injection in combination with closing of fractured zones result in high oil production and good distribution of CO_2 in the reservoir.

References

Kamal Ahmed, CO_2 injeksjon for økt oljeutvinning i kalk, *Masteroppgave, Institutt for fysikk og teknolo*gi, Universitet i Bergen, 2013.

China Oilfield Technology, Annual report 2013, Available from: http://www.chinaoilfieldtech.com/oilrecovery.html

Glenn-Andre Dåtland Kvinge, En eksperimentell studie av CO_2 lagring i sandstein og kalkstein med bruk av ulike avbildningsteknikker, *Masteroppgave, Institutt for Fysikk og teknologi, Universitet i Bergen*, 2012.

Amin Ettehadtavakkol, Larry W. Lake and Steven L. Bryant, CO_2-EOR and storage design optimization, *International Journal of Greenhouse Gas Control*, Vol. 25: p. 79-92, June 2014.

E. Ghoodjani and S.H. Bolouri, Experimental study and calculation of CO_2-oil relative permeability, *Petroleum & Coal*, ISSN 1337-7027, 53-(2) : p. 123-131, Sharif University of Technology, Shahid Bahonar University, Kerman, Iran, 2011.

Bruce Hill, Susan Hovorka and Steve Melzer, Geologic carbon storage through enhanced oil recovery, *Energy Procedia*, vol. 37: p. 6808-6830, Elsevier Ltd., USA, 2013

HIS Energy, Available from: *http://www.fekete.com/SAN/WebHelp/FeketeHarmony/Harmony_WebHelp/Content/HTML_Files/Reference_Material/General_Concepts/Relative_Permeability.htm*.

Norman J. Hyne, Ph.D., Nontechnical Guide to Petroleum Geology, Exploration, Drilling and Production, *Penn Well Corporation*, Second edition, ISBN: 0-87814-823-X, USA, 2001.

Viktor E. Jakobsen, F.H., Marius Holm, Beate Kristiansen, BELLONA, *CO2 for EOR on the Norwegian shelf -A case study*. 2005: p. 108.

Kamal Jawher Khudaida and Diganta Bhusan Das, A numerical study of capillary pressure-saturation relationship for supercritical carbon dioxide (CO_2) injection in deep saline aquifer, *Chemical Engineering research and Design*, Volume 92, Issue 12: p. 3017-3030, Desember 2012.

Madhav M. Kulkarni, Immiscible and miscible gas-oil displacements in porous media, *Master thesis, Graduate Faculty of the Louisiana State University and Agricultural and Mechanical College*, India, 2003.

Stephen L. Melzer, Carbon Dioxide Enhanced Oil Recovery (CO_2EOR): Factors Involved in Adding Carbon Capture, Utilization and Storage (CCUS) to Enhanced Oil Recovery, *CO_2 Consultants and Annual CO_2 Flooding Conference Director*, Midland,Tx, February 2012

NETL/DOE, *Carbon Dioxide Enhanced Oil Recovery - Untapped Domestic Energy Supply and Long Term Carbon Storage Solution.* 2010.

NRG Fact Sheet, CO_2 Enhanced Oil Recovery, *NRG Energy Inc.*, Texas, 2014, Available from: http//www.nrgenergy.com

Oljeindustriens Landsforening, Innføring i Geologi, Faktahefte for Utdanning til olje og gassindustrien, Available from: *http://www.utog.no/postmann/dbase/bilder/geologihefte-web.pdf*

Sangeeta M. Pasala, CO2 displacement mechanisms: Phase equilibria effects and Carbon dioxide sequestration studies, *PhD, Department of Chemical Engineering, The University of Utah*, December 2010.

Richard C. Selley, Elements of Petroleum Geology, *Academic Press California*, second edition, ISBN: 0-12-636370-6 USA, 1998.

Rocky Mountain Carbon Capture and Sequestration, available from: *http://rmccs.org/sitecharacterization/experimental3.html*

Schlumberger, Fundamentals of Wettability, *Oilfield Review*, Volume 19, Number 2: p. 66-71, summer 2007.

Djebbar Tiab and Erle C. Donaldson, Petrophysics, Theory and Practice of Measuring Reservoir Rock and Fluid Transport Properties, *Gulf Professional Publishing*, Third edition, ISBN: 978-0-12-383848-3, USA, 2012.

Appendix C

Simulation of oil production in a water-wet carbonate reservoir

Table C-1: Specifications for simulation of water-wet cases.

	Case C1	**Case C2**
Water-wet Reservoir	Open valve Without CO_2-injection	Open valve With CO_2-injection

Corey's coefficient

Table C-2: Corey coefficient in water-wet reservoirs. [37]

Wettability	**n_w**	**n_{ow}**
Water-wet	2-4	6-8

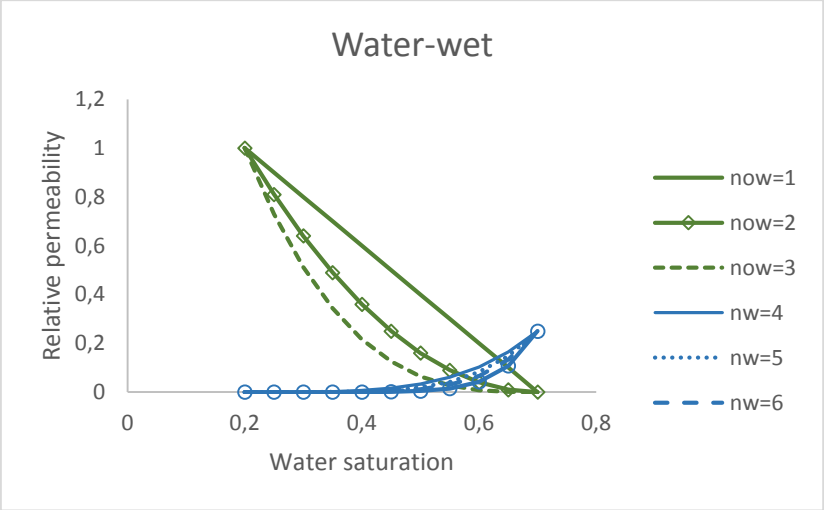

Figure C-1: Oil and water relative permeability curves for a water-wet reservoir, with variable values for the Corey coefficient.

Input to OLGA/Rocx

Table C-3: Relative permeability data for the specific cases.

	Water-Wet	
S_{wc}	0.2	0.2
S_{or}	0.3	0.2
K_{rowc}	1	1
K_{rwoc}	0.25	0.25
n_w	8	8
n_{ow}	2	2

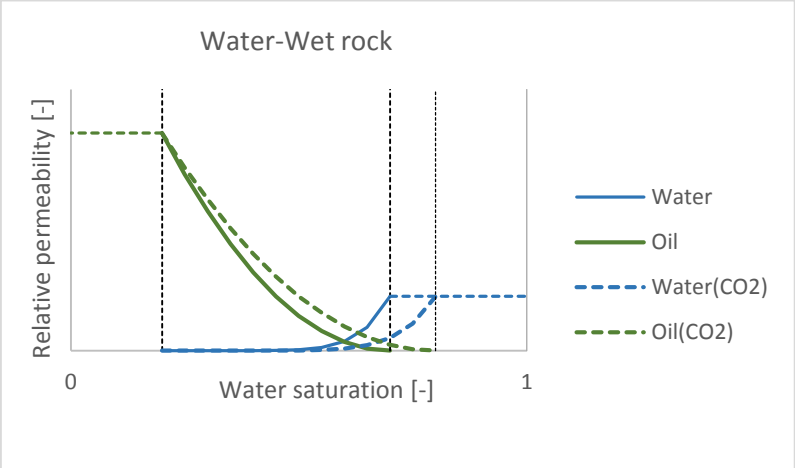

Figure C-2: Relative permeability curves in oil-wet reservoir.

Table C-4: Input for the specific simulation cases.

Simulation Case	Data input to Rocx	Relative permeability curve	CO2-injection	Position Valve A and C	Position Valve B
Case 5	See Table 5-1	Figure A-2	No	Open	Open
Case 6	See Table 5-1	Figure A-2	Yes	Open	Open

Results

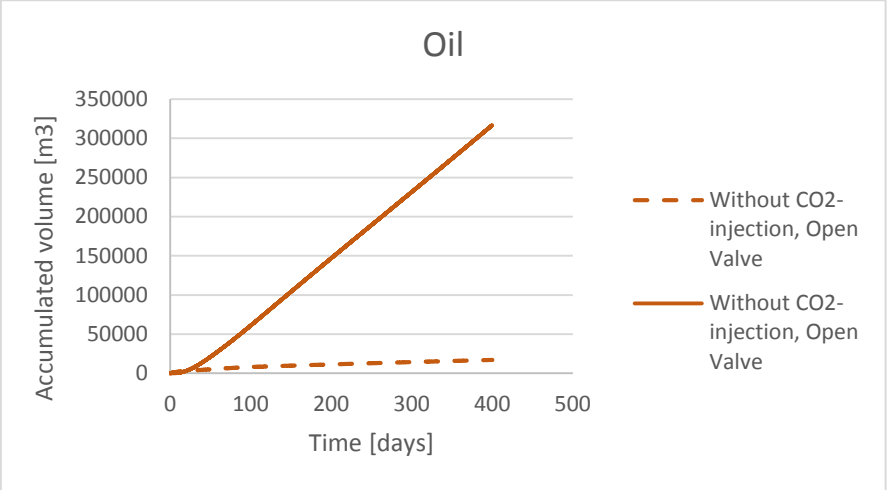

Figure C-3: Accumulated oil in oil-wet reservoir.

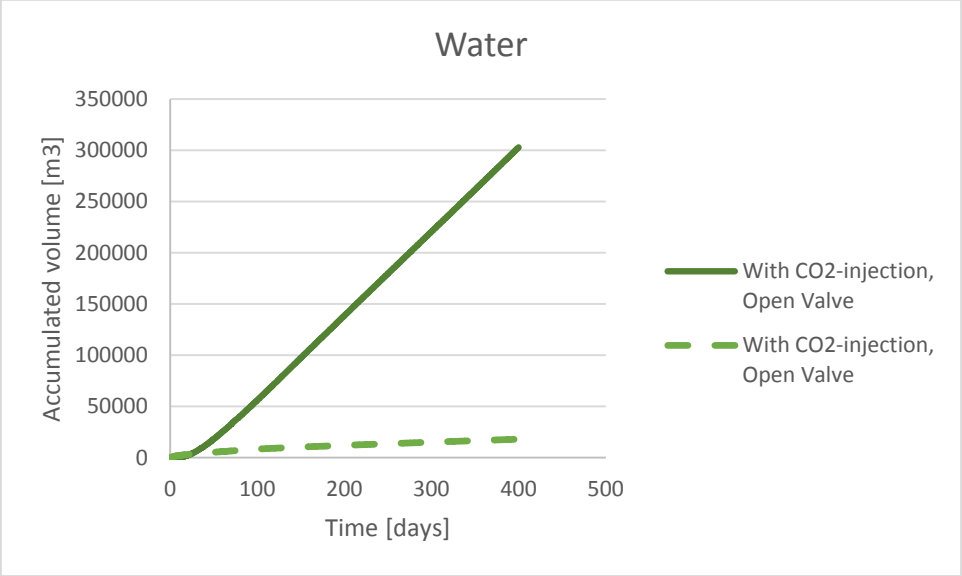

Figure C-4: Accumulated water in oil-wet reservoir.

Appendix D

Calculation of Relative Permeability Boost Factor for Oil. [37]

Relative Permeability Boost Factor

$$RBF_O = \sqrt{\frac{(IFT_{CO2}) \cdot (\mu_{O,CO2}) \cdot (SF_{N2})}{(IFT_{N2}) \cdot (\mu_{O,N2}) \cdot (SF_{CO2})}} \qquad [D\text{-}1]$$

Input data

Table D-1: Effect of CO_2 and N_2 on IFT, oil viscosity and swelling factor.

	IFT	Oil viscosity	Swelling factor
Initial	11.868	1.0509	1
N2	11.842	1.0503	1.0001
CO2	8.639	0.735	1.1022

Table D-2: Ratio of residual oil saturation and Corey's exponent for oil relative permeability.

	$\frac{S_{or,CO2}}{S_{or,N2}}$	$\frac{n_{o,CO2}}{n_{o,N2}}$
Test 1	0.74857	0.519909
Test 2	0.76667	0.686395
Test 3	0.72	0.604524
Equals	$\sqrt{RBF_o} = 0.754288$	$RBF_o = 0.568951$

Correlation factor

$$n_{o,CO2} = RBF_o \cdot n_{o,N2} \rightarrow n_{o,CO2} = 0.568951 \cdot n_{o,N2} \quad \textit{[D-2]}$$

$$S_{or,CO2} = \sqrt{RBF_o} \cdot S_{or,N2} \rightarrow S_{or,CO2} = 0.754288 \cdot S_{or,N2} \quad \textit{[D-3]}$$